의학박사 학위논문

A Combination Treatment of Glycolytic Inhibitor and Reactive Oxygen Stress Enhancer in Sorafenib-resistant and High Metastatic Potential Hepatocellular Carcinoma Cells

간암에서 소라페닙 저항성 및 전이성 세포에 대한 해당과정 억제제 및 활성산소 촉진제의 병용치료 효과

2016 년 2 월

서울대학교 대학원

임상의과학과 전공

이 민 종

A thesis of the Degree of Doctor of Philosophy

간암에서 소라페닙 저항성 및 전이성 세포에 대한 해당과정 억제제 및 활성산소 촉진제의 병용치료 효과

A Combination Treatment of Glycolytic Inhibitor and Reactive Oxygen Stress Enhancer in Sorafenib-resistant and High Metastatic Potential Hepatocellular Carcinoma Cells

February 2016

The Department of Clinical Medical Sciences,

Seoul National University

College of Medicine

Minjong Lee

A Combination Treatment of Glycolytic Inhibitor and Reactive Oxygen Stress Enhancer in Sorafenib-resistant and High Metastatic Potential Hepatocellular Carcinoma Cells

by

Minjong Lee, M.D

A thesis submitted to the department of
Clinical Medical Sciences, Graduate School in
partial fulfillment of the requirements
for the Degree of Doctor of Philosophy
in Clinical Medical Sciences at the
Seoul National University College of Medicine

December 2015

Approved by Thesis Committee:

Professor _____ **Chairman**

Professor _____ **Vice chairman**

Professor _____

Professor _____

Professor _____

ABSTRACT

BACKGROUND & AIM: Acquisition of anoikis resistance (AR) is a prerequisite for the metastasis in hepatocellular carcinoma (HCC). However, little is known about how energy metabolism and antioxidant system are changed in HCC AR cells. We aimed to evaluate the anti-tumor effect of a combination treatment of 3-bromopyruvate (3-BP), an inhibitor for glycolysis, and buthionine sulfoximine (BSO), an inhibitor for glutathione synthesis in HCC AR cells.

METHODS: We compared glycolysis, reactive oxygen species (ROS) production, and chemoresistance among Huh-BAT, HepG2 human HCC cells, and corresponding AR cells. Expression of hexokinase II, gamma-glutamylcystine synthetase (rGCS), and epithelial–mesenchymal transition markers in AR cells was assessed. Anti-tumor effect of a combination treatment of 3-BP and BSO were evaluated in AR cells and HCC xenograft mouse model.

RESULTS: AR cells showed a significantly higher chemoresistance, glycolysis, and lower ROS production than attached cells. Expression of hexokinase II, rGCS, and Snail was higher in HCC AR cells than attached cells. A combination treatment of 3-BP and BSO effectively suppressed proliferation of HCC AR cells through apoptosis induction by blocking glycolysis and enhancing ROS levels. In a xenograft mouse model, tumors induced from HCC AR cells more rapidly grew than HCC attached cells. Growth rates of tumors derived from HCC AR cells were significantly suppressed in the group treated with 3-BP and BSO as compared to the group treated with 3-BP or sorafenib alone.

CONCLUSIONS: These results demonstrate that a combination treatment of 3-BP and BSO has a synergistic anti-tumor effect in HCC AR model. This strategy might be an effective adjuvant therapy to patients with sorafenib-resistant HCC.

Key words; 3-bromopyruvate; buthionine sulfoximine; Hepatocellular carcinoma; Anoikis-resistant cell

Student Number: 2014-30915

CONTENTS

LIST OF TABLES AND FIGURES

No Table

Figure 4. Change of intracellular lactic acid and ROS production after matrix detachment. (A) Lactic acid production in Huh-BAT AR and HepG2 AR cells was significantly increased than that in Huh-BAT and HepG2 cells: $P<0.001$ for Huh-BAT AR cell and $P<0.001$ for HepG2 AR cell. (B) ROS production in Huh-BAT AR and HepG2 AR cells was significantly decreased than that in Huh-BAT and HepG2 cells: $P=0.039$ for Huh-BAT AR cells and $P=0.021$ for HepG2 AR cells.

* means $P<0.05$; *** means $P<0.001$.

Abbreviation: AR, anoikis resistant; ROS, reactive oxygen species.

Bars, SD.

Figure 5. Chemoresistance phenotype of the HCC AR cells as compared to HCC attached cells. (A) Huh-BAT AR cells showed significantly higher viabilities at 3 μM of sorafenib, 1 μM of 5-FU, and 10 μM of cisplatin as compared to Huh-BAT cells. (B) HepG2 AR cells showed significantly higher viabilities at 3 μM of sorafenib and 1 μM of 5-FU as compared to HepG2 cells. (C) Huh-BAT AR and (D) HepG2 AR cells showed significantly higher viabilities at concentration of 5 and 10 μM of sorafenib as compared to Huh-BAT and HepG2 cells.

* means $P<0.05$; ** means $P<0.01$.

Abbreviation: AR, anoikis resistant; sora, sorafenib; 5-FU, 5-fluorouracil.

Bars, SD.

Figure 6. Rapid tumor growth in xenograft nude mice bearing Huh-BAT AR cells. Tumor growth rates of Huh-BAT AR cells were significantly higher than those of Huh-BAT cells ($P=0.026$).

Abbreviation: AR, anoikis resistant.

Figure 7. Expression of HK II and rGCS after 3-BP, BSO, and a combination treatment of 3-BP and BSO in Huh-BAT, HepG2, and corresponding AR cells. (A) Expression of HK II was decreased after 3-BP (40 μM) treatment and increased after BSO (200 μM) treatment; Expression of rGCS was increased after BSO (200 μM) treatment. (B) When treated with a combination treatment of 3-BP (40 μM) and BSO (200 μM), HK II expression was suppressed and rGCS expression was increased as compared to the control.

Abbreviation: AR, anoikis resistant; BSO, buthionine sulfoximine; CTL, control; HK II, hexokinase II; rGCS, gamma-glutamylcysteine synthetase; 3-BP, 3-bromopyruate.

Figure 8. Suppression of glutathione production. Glutathione production was significantly suppressed after BSO or a combination treatment of 3-BP (40 μM) and BSO (200 μM) as compared to the control in Huh-BAT AR and HepG2 AR cells: $P<0.001$, BSO; $P<0.001$, a combination treatment for Huh-BAT AR cells and $P=0.001$, BSO; $P=0.001$, a combination treatment for HepG2 AR cells.

* means $P<0.05$; ** means $P<0.01$; *** means $P<0.001$

Abbreviation: AR, anoikis resistant; BSO, buthionine sulfoximine; 3-BP, 3-bromopyruate.

Figure 9. Change of ROS production by 3-BP (40 μM), BSO (200 μM), or a combination treatment of 3-BP and BSO. *In situ* fluorescence staining showed high enhancement in cells treated with the indicated treatment as compared to the control in Huh-BAT AR (A) and HepG2 AR cells (B). (C) ROS production was significantly increased at 3-BP (40 μM), BSO (200 μM), and a combination treatment of 3-BP (40 μM) and BSO (200 μM) as compared to the control ($P=0.003$, 3-BP; $P=0.02$, BSO; $P=0.002$, a combination treatment of 3-BP and BSO for Huh-BAT AR cells and $P<0.001$, 3-BP; $P=0.008$, BSO; $P=0.003$, a combination treatment of 3-BP and BSO for HepG2 AR cells).

Abbreviation: AR, anoikis resistant; BSO, buthionine sulfoximine; ROS, reactive oxygen species; 3-BP, 3-bromopyruate.

Figure 10. Change of lactic acid production by 3-BP (40 μM), BSO (200 μM), and a combination treatment of 3-BP and BSO. (A) Lactic acid production in Huh-BAT, HepG2, and corresponding AR cells was significantly suppressed after 3-BP (40 μM) treatment as compared to the control (P=0.038 for Huh-BAT; P<0.001 for Huh-BAT AR; P<0.001 for HepG2; P=0.002 for HepG2 AR cells). (B) Lactic acid production in Huh-BAT, HepG2, and corresponding AR cells was significantly increased after BSO (200 μM) treatment as compared to the control (P<0.001 in Huh-BAT; P<0.001 in Huh-BAT AR; P<0.001 in HepG2; P=0.001 in HepG2 AR cells). (C) Lactic acid production was significantly suppressed after a combination treatment of 3-BP (40 μM) and BSO (200 μM) in Huh-BAT AR and HepG2 AR cells; there was a significant difference among baseline, 2, and 12 hours exposure to a combination treatment (P<0.001 between baseline and 2 hours and P<0.001 between baseline and 12 hours exposure in Huh-BAT AR cells; P=0.042 between baseline and 2 hours and P=0.01 between baseline and 12 hours exposure in HepG2 AR cells).

* means P<0.05; ** means P<0.01; *** means P<0.001

Abbreviation: AR, anoikis resistant; BSO, buthionine sulfoximine; ROS, reactive oxygen species 3-BP, 3-bromopyruate.

Bars, SD.

Figure 11. Cell viabilities of Huh-BAT, HepG2, and corresponding AR cells after 3-BP or BSO treatment. (A) Viabilities of Huh-BAT and Huh-BAT AR cells were decreased after 3-BP treatment. (B) In Huh-BAT AR cells, cell viabilities at each concentration were significantly lower after BSO treatment as compared to those of Huh-BAT cells (all, P<0.05).

(C) Viabilities of HepG2 AR cells showed significantly higher than those of HepG2 cells after 3-BP treatment (all, P<0.01). (D) In HepG2 and HepG2 AR cells, cell viabilities were not effectively suppressed after BSO treatment. At high concentration of 800 μM, BSO, viabilities of HepG2 AR cells were significantly suppressed as compared to those of HepG2 cells (P=0.04).

* means P<0.05; ** means P<0.01; *** means P<0.001

Abbreviation: AR, anoikis resistant; BSO, buthionine sulfoximine; 3-BP, 3-bromopyruate.

Bars, SD.

Figure 12. Cell viabilities of Huh-BAT, HepG2, and corresponding AR cells after a combination treatment of 3-BP and BSO. Viabilities of Huh-BAT and Huh-BAT AR cells (A), HepG2 and HepG2 AR cells (B) were effectively suppressed. Each concentration of 3-BP was treated 24 hours after 200 μM BSO treatment in those cells.

** means P<0.01

Abbreviation: AR, anoikis resistant; BSO, buthionine sulfoximine; 3-BP, 3-bromopyruate.

Bars, SD.

Figure 13. Apoptosis assay after 3-BP, BSO, and a combination treatment of 3-BP and BSO. Apoptosis rates of Huh-BAT, HepG2, and corresponding AR cells receiving the indicated treatments were evaluated by annexin V-FITC staining. The upper panel depicts the proportion of apoptotic cells, and the lower panel shows the quantitative results. A combination treatment of 3-BP and BSO significantly increased apoptosis rates as compared to the control (P=0.026 in Huh-BAT; P=0.001 in Huh-BAT AR; P=0.004 in HepG2; P=0.002 in HepG2 AR cells). When apoptosis rates were compared according to each treatment, a combination treatment of 3-BP and BSO showed higher apoptosis rates as compared to single treatment of 3-BP or BSO;

P=0.012, 3-BP in Huh-BAT cells; P=0.002, BSO and P=0.001, 3-BP in Huh-BAT AR cells; P=0.001, BSO and P=0.002, 3-BP in HepG2 cells; P=0.002, BSO and P=0.001, 3-BP in HepG2 AR cells. 3-BP concentrations, 40 μM were used for Huh-BAT/Huh-BAT AR cells and 60 μM for HepG2/HepG2 AR cells; BSO concentrations, 200 μM were used for all indicated cell lines.
* means P<0.05; ** means P<0.01
Abbreviation: AR, anoikis resistant; BSO, buthionine sulfoximine; 3-BP, 3-bromopyruate.
Bars, SD.

Figure 14. Suppression of HCC invasion by 3-BP, BSO, a combination treatment of 3-BP and BSO. Invasion capability of Huh-BAT AR and HepG2 AR cells receiving the indicated treatments was examined by Boyden chamber assay (A and C) and the bar graph depicts quantification of migrated cells (B and D). Invasion capability of Huh-BAT AR (B) and HepG2 AR cells (D) receiving the indicated treatments was significantly lower from the control; the combined 3-BP (40 μM) with BSO (200 μM) treatment in either Huh-BAT AR or HepG2 AR cells significantly suppressed cell invasion as compared with the control (P=0.002, 3-BP; P=0.001, BSO; P=0.001, a combination treatment for Huh-BAT AR cell and P=0.006, 3-BP; P<0.001, BSO; P<0.001, a combination treatment for HepG2 AR cell).
* means P<0.05; ** means P<0.01; *** means P<0.001
Abbreviation: AR, anoikis resistant; BSO, buthionine sulfoximine; 3-BP, 3-bromopyruate.
Bars, SD.

Figure 15. In vivo anti-tumor effects of 3-BP, sorafenib, and a combination treatment of 3-BP and BSO in xenograft nude mice bearing Huh-BAT AR cells. (A) Tumor growth rates in a combination treatment group were significantly lower than those in the control, sorafenib, or 3-BP treatment group (P=0.008, P=0.011, and P=0.013, respectively)(upper panel). There was

no significant difference of tumor growth rates between the control and sorafenib treatment group (P=0.437), or between the control and 3-BP treatment group (P=0.243). Gross pictures of tumors before treatment, tumors grown in the control group, and tumors in a combination treatment group were shown (lower panel). (B) In vivo demonstration of the apoptosis-inducing efficacy in the control, 3-BP, sorafenib, and a combination treatment group was shown: H&E and TUNEL staining of tumor tissues in the control, sorafenib, 3-BP, and combination-treated mice (x 40 magnification). (C) TUNEL-positive cell percentages (apoptotic index) were determined in six different high power (x 400 magnification) fields. Apoptotic index was significantly higher in a combination treatment group as compared to other groups (P<0.001, the control group; P=0.001, the sorafenib treatment group; P=0.004, the 3-BP treatment group). (D) There was a significant difference of body weight between the control group and a combination treatment group (P=0.021).

* means P<0.05; ** means P<0.01; *** means P<0.001

Abbreviation: AR, anoikis resistant; BSO, buthionine sulfoximine; 3-BP, 3-bromopyruate.

Bars, SD.

Figure 16. After matrix detachment, anoikis-resistant cancer cells decrease intracellular ROS levels through inducing enzymes involved in the glycolysis and antioxidant systems for their survival. The Warburg effect can be modulated by increased intracellular ROS levels. Increased ROS levels induce HK II expression and make cancer cells sensitive to 3-BP treatment, and thereby promote cell death via ROS-mediated apoptosis (the black box indicates monocarboxylate transporter 1, and the white box indicates monocarboxylate transporter 4).

Abbreviation: HK II, hexokinase II; ROS, reactive oxygen species; 3-BP, 3-bromopyruate.

LIST OF ABBREVIATIONS

AR: anoikis-resistant cell

BSO: buthionine Sulfoximine

CSC: cancer stem cell

CTL: control

DMEM: Dulbecco modified Eagle medium

FBS: fetal bovine serum

rGCS: gamma-glutamylcysteine synthetase

EMT: epithelial–mesenchymal transition

HCC: hepatocellular carcinoma

HIF: Hypoxia-inducible factor

HK II: hexokinase II

MnSOD: manganese superoxide dismutase

NF-kB: nuclear factor kappa-light-chain-enhancer of activated B cells

OXPHOS: oxidative phosphorylation

PI3K: Phosphatidylinositol-4,5-bisphosphate 3-kinase

Poly-HEMA: Poly-hydroxyethylmethacrylate

p-PDH: phosphorylated pyruvate dehydrogenase

ROS: reactive oxygen species

TUNEL: terminal deoxynucleotidyl transferase-mediated dUTP nick end labeling

3-BP: 3-bromopyruvate

5-FU: 5-fluorouracil

Introduction

Hepatocellular carcinoma (HCC) is the fifth leading cancer in men and the seventh leading cancer in women with a total of 0.7 million new cases worldwide (1). Although curative treatments such as surgical resection, liver transplantation, and local ablation can significantly improve the survival of HCC patients at the early stage (2, 3), HCC recurs in 70% of patients at 5 years and includes either intrahepatic metastases or the development of de novo tumors (4, 5). To patients with advanced HCC, only sorafenib significantly prolonged patients' survival in advanced HCC until now. However, the long-term survival benefit from sorafenib treatment is the modest improvement of 3 months far from satisfactory (6). Some other anti-angiogenesis drugs have been evaluated preclinically and clinically for the treatment of HCC, but their effects were not competitive (7). Therefore, new targeting agents beyond anti-angiogenesis should be needed for alternative treatments in patients with advanced HCC who did not respond to sorafenib or anti-angiogensis agents.

Metastasis is a multistep process including dissociation of cancer cells from primary sites, survival in the vascular system, and proliferation in distant target organs. As a barrier to metastasis, cells normally undergo an apoptotic process known as "anoikis," a form of cell death due to loss of contact with the extracellular matrix or neighboring cells (8-10). Cancer cells acquire anoikis resistance (AR) to survive after detachment from primary sites and travel through the circulatory and lymphatic systems to disseminate throughout the body (11).

Previous studies reported the charactertics of AR cells; a high capability of metastasis; chemoresistance to conventional drugs such as 5-fluorouracil, cisplatin, and mitoxantrone (12, 13); rapid growing pattern as compared to anoikis-sensitive cancer cells. Although the underlying mechanism of survival in HCC AR cells was not fully investigated, glycolysis and antioxidant systems modulating intracellular reactive oxygen species (ROS) levels have been suggested as key players for survival; AR cells potentiates glycolysis for effective energy

production under limited sources and activates antioxidant systems for prevention of ROS-mediated apoptosis under detached condition (14).

With regard to relation between glycolysis and ROS production, acceleration of glycolysis in cancer cell energy metabolism, i.e. the Warburg effect, reduces the ROS production by less dependence on mitochondrial oxidative phosphorylation (OXPHOS). In addition, increased glucose consumption diverts more glucose carbon into the oxidative branch of the pentose phosphate pathway, which represents a major source to generate NADPH and materials for DNA biosynthesis in proliferative cancer cells (15). NADPH is a critical cofactor for the replenishment of reduced glutathione (GSH) in a cell. When oxidative stress increases in cancer cells, antioxidant generation pathway can be activated via pyruvate kinase M2 inhibition (16). This inhibition of PKM2 is required to divert glucose flux into the pentose phosphate pathway which provides NADPH required for glutathione reductase to generate GSH for ROS detoxification (16).

This contribution of the Warburg effect to intracellular redox balance can play a pivotal role to initiate metastasis in AR cell, i.e., matrix detachment. In normal cells, mitochondrial OXPHOS is attenuated in response to matrix detachment for their survival. Pyruvate dehydrogenase kinase (PDK) 4 is activated to inhibit pyruvate dehydrogenase (PDH) to upregulate glycolytic pathway in normal cell response following detachment. However, many cancer cells already upregulate glycolysis and attenuate mitochondrial OXPHOS even under adherent status because of the Warburg effect. Cancer cells also express high levels of PDK 1 before detachment for effective energy metabolism for their survival (14). Intesrestingly, in patients' prognosis, PDK expression in various cancers significantly correlates with tumor histological grades and disease-free survival (17, 18). PDK inhibition (PDH activation) in cancer cells activates mitochondrial OXPHOS and increases ROS production. Increase of intracellular ROS levels activates cancer cells' susceptibility to apoptosis after matrix

detachment, which leads to a decreased metastatic potential (14). Therefore, the Warburg effect indirectly allows cancer cells to lower ROS production by less reliance on mitochondrial OXPHOS for glucose metabolism (19). Reduction of ROS levels, which promotes metastasis, may represent an advantage given by the Warburg effect.

In addition to the Warburg effect, the vulnerability for oxidative stress in normal and cancer cells is quite different. Cancer cells can potentiate antioxidant systems itself to cope with increased oxidative stress (15). In cancer cells, increased ROS production from metabolic dysregulation and rapid proliferation may induce upregulation of antioxidant capacity: vulnerable redox equilibrium with high ROS production and elimination to maintain the ROS levels below the threshold for cell death (20, 21). Enhanced antioxidant capacity allows cancer cells to better survive detachment-induced oxidative stress and initiate to metastasize. In a animal model for lung cancers, antioxidant treatments have consistently reduced oxidative stress and accelerated lung cancer progression (22). Increased expression of manganese superoxide dismutase (MnSOD) in cancers was significantly associated with aggressive phenotypes of cancers in previous stuides (23-25). In contrast, normal cells have tolerability for a certain level of exogenous ROS stress because of their high antioxidant capacity for lowering the ROS levels and thereby prevent to reach the cell-death threshold (26, 27). Normal cells have high buffering capacity to activate MnSOD expression after matrix detachment (23): more tolerable to oxidative stress than cancer cells. Thus, cancer cells could be more vulnerable to increased oxidative stress induced by exogenous ROS enhancers that directly or indirectly suppress the antioxidant system (28-31).

Until now, many previous studies have showed anti-tumor effects of the glycolytic inhibitors in HCC experimental models; suppression of tumor growth such as 3-bromopyruvate (3-BP) (32-42), 3-bromo-2-oxopropionate-1-propyl ester (43), dichloroacetate (44, 45), lonidamine (46), methyl jasmonate (47-49), and 3-(3-pyridinyl)-1-(4-pyridinyl)-2-propen-1-one (50).

Among various glycolytic inhibitors, only 3-BP could target two energy machineries such as glycolysis and mitochondrial OXPHOS. The mechanism for potent anti-tumor effects of 3-BP indicated that mitochondrion-bound hexokinase II (HK II) was essential for the high glycolytic capacity using mitochondrial ATP rather than cytosolic ATP, and lowering of mitochondrial OXPHOS capacity by attenuating Pi and ADP delivery to the mitochondria (51, 52).

Of note, with the exception of 3-BP, there are four common characteristics in previous studies which have reported the anticancer effects of these glycolytic inhibitors: (i) not strong anti-tumor effects when used alone; (ii) synergistic or additive anti-tumor effects of other chemotherapy agents, such as 5-fluorouracil, cisplatin, doxorubicin, and sorafenib when used with the glycolytic inhibitors; (iii) a sensitizer to make cancer cells vulnerable to radiotherapy and photodynamic therapy; and (iv) an enhancer of oxidative stress to induce apoptosis in cancer cells (53).

Considering the relation of the Warburg effect with ROS attenuation, differences of defense capability for oxidative stress between normal and cancer cells, and change of ROS levels in process of metastasis initiation, the fourth characteristic of the glycolytic inhibitors, "an enhancer of oxidative stress", can suggest a rationale for a combination treatment of glycolytic inhibitors and exogenous ROS enhancers. A further increase in ROS stress using exogenous ROS enhancers combined with glycolytic inhibitors might effectively increase ROS levels above the threshold stimulating cell death pathways and deplete enery production of cancer cells mainly dependent on glycolysis

Although previous studies showed that the Warburg effect and ROS suppression are closely linked each other for cancer cell survival, particularly AR cells, there have been lack of stuides for a combination treatment of specific inhibitors for the Warburg effect and ROS suppression in HCC AR cells. In the glycolysis pathway, expression of HK II, the first step enzyme rate-limiting, is significantly correlated with lactic acid production which is the end product of

glycolysis (52). In cancer cells in hypoxia, anti-tumor effects of 3-BP, an HK II inhibitor, has well-established (54). In antioxidant system in cancer cells, glutathione plays a crucial role to reduce the intracellular ROS level. Glutathione levels and expression of GSH synthetase in HCC were higher as compared to normal liver (55). In production of glutathione, gamma-glutamylcysteine synthetase (rGCS) is the first and rate-limiting enzyme (56-58). Buthionine sulfoximine, an irreversible inhibitor for rGCS, showed significantly elevation of intracellular ROS levels and thereby induced apoptosis by cytochorme c and caspase 3 activation (56, 59).

In the present study, we aimed to clarify the characteristics of HCC AR cells induced from human hepatocellular carcinoma cell lines with focus on HK II, rGCS expression, chemoresistance to sorafenib and invasion capabilities, and anti-tumor effects of a combination treatment of each inhibitor for glycolysis and antioxidant systems in HCC AR cells.

Materials and Methods

Cell Culture and Reagents

Human hepatocellular carcinoma cell lines, Huh-BAT and HepG2 cells were obtained from Korea Cell Line Bank and cultured in Dulbecco's modified Eagle's medium (DMEM) (DMEM; Life Technologies, Grand Island, NY) containing 10% fetal bovine serum (FBS, Life Technologies). Cells were incubated at 37℃ in a humidified atmosphere containing 5% CO2. For adherent culture, HCC attached cells were grown on the tissue culture dishes (Falcon, San Jose, CA), while for suspension culture, cells were grown on dishes coated with 10 mg/ml Poly-hydroxyethylmethacrylate (Poly-HEMA) (Sigma, St. Louis, MO). To select cells that could survive in suspended culture, 1×10^6 cells were seeded on Poly-HEMA coated dishes and grown for 28 days. Fresh media were added every 3 days. After 7 days in culture, cells were harvested and treated with diluted trypsin-EDTA (GibcoBRL, Grand Island, NY) to obtain a single-cell suspension for re-plating or trypan blue exclusion assay. We defined the suspended cells as anoikis-resistant (AR) cells; Huh-BAT AR and HepG2 AR cells were induced from Huh-BAT and HepG2 attached cells, respectively.

For experiments comparing HCC attached cells and AR cells, 5×10^5 cells were seeded in appropriate culture dishes, grown for 48 hours, harvested, treated with diluted trypsin-EDTA, and analyzed as indicated. In a set of experiments, cells were incubated for 72 hours with media containing each compound; 40 μM 3-BP (Sigma, St. Louis, MO); 200 μM BSO (Santa Cruz, Dallas, Texas); 3 μM, Sorafenib (LC Laboratories, Woburn, MA); 1 μM, 5-fluorouracil (5-FU) (Sigma, St. Louis, MO); 10 μM, cisplatin (Sigma, St. Louis, MO); 10 nM, doxorubicin (Sigma, St. Louis, MO). Cell viability was determined by incubating cells with 0.4% trypan blue dye. Cells were then counted with 0.4% trypan blue dye in a Neubauer chamber.

Western Blot Analysis

Human hepatocellular carcinoma cells were collected and lysed in lysis buffer (150 mM sodium chloride, 1% tritionX-100, 1% sodium deoxycholate, 0.1% sodium dodecyl sulfate, 50 mM tris-HCl [pH 7.5], 2 mM EDTA, protease inhibitor cocktail). Then, proteins were quantified with a BCA protein assay kit (Thermo, Rockford, IL). Equal amounts of protein were loaded onto a SDS-polyacrylamide gel (10% polyacrylamide) followed by electrophoresis at 100 V for 3 hours and transferred to poly-vinylidene floride (PVDF) membrane at 50 V for 2 hours. The PVDF membrane incubated 4℃ overnight with the target primary antibody. Anti-HK II (Santa Cruz, Dallas, Texas), rGCS (Santa Cruz, Dallas, Texas), phosphorylated pyruvate dehydrogenase (Abcam, Cambridge, MA), Snail (Cell Signaling Technology, Danvers, MA), E-cadherin (Cell Signaling Technology, Danvers, MA), and β-actin (Santa Cruz, Dallas, Texas) antibodies were diluted in TBS-T (TBS/Tween 20: 2% skim milk). The secondary antibodies (horseradish peroxidase-conjugated anti-rabbit and mouse) were applied at room temperature for 1 hour. Immunoreactivity was developed using a peroxidase conjugate antiserum (Santa Cruz, Dallas, Texas) and detected by enhanced chemiluminescence reagents (Promegaison, WI). Western blotting of Huh-BAT, HepG2, Huh-BAT AR, and HepG2 AR cells treated with 40-60 μM of 3-BP (Sigma-Aldrich) alone, 200 μM of BSO (Santa Cruz, Dallas, Texas) alone, or combined 40-60 μM of 3-BP with 200 μM of BSO was performed.

Measurement of Intracellular Lactic Acid Levels

Intracellular lactic acid levels were measured using lactate assay kit (BioVision, Milpitas, CA). The assay was performed following the manufacturer's instructions. For experiments with 40 μM of 3-BP or 200 μM of BSO, the cells were pretreated as described above. The relative concentrations were normalized to the cell number of each sample. Briefly, cells were

homogenized in lactate assay buffer and deproteinized with 10 kDa spin filters to remove insoluble material. The lactate concentration was measured at 535/590 nm using a multiwall plate reader. Experiments were performed in triplicate.

Measurement of Intracellular Glutathione Levels

Intracellular total glutathione levels were quantified with a glutathione fluorometric assay kit (BioVision, Milpitas, CA) by following manufacture's instruction. Briefly, after cells were treated with 40 µM of 3-BP or 200 µM of BSO for 48 hours, 1×10^6 cells were homogenized in PCA on ice for 5 minutes and centrifuged at 13,000 g for 2 minutes. The supernatants were collected, and 20 µl of cold KOH was added to neutralize the samples. Neutralized samples were transferred to a 96-well plate for detection on a fluorescence plate reader equipped with fluorometric absorbance at 340/420 nm. Experiments were performed in triplicate.

Detection of Intracellular ROS Production

Intracellular ROS levels were determined using the ROS/RNS assay kit (Abcam, Cambridge, MA) which was based on DCFH probe. Cells were treated with 40 µM of 3-BP or 200 µM of BSO and collected in PBS. Cell lysates were added into a 96-well black plate. Then, catalyst was added into all test wells. Samples were mixed well and incubated 5 minutes at room temperature. The DCFH solution was added into all test wells and incubated at room temperature for 30 minutes. The fluorescence was read at 480 nm excitation/530 nm emission. To visualize, cells were dyed through fluorescent dye reagents. Upon staining, the fluorescent products generated by the dye can be visualized using a wide-field fluorescence microscope equipped with standard red (Ex/Em=650/670 nm) fluorescent cubes. Experiments were performed in triplicate.

Apoptosis Determination

HCC cells were cultured and divided into 4 groups according to the treatment: (i) control, (ii) 3-BP alone, (iii) BSO alone, and (iv) a combination treatment of 3-BP and BSO. After trypsinization, the cells were incubated with 8 μl annexin V-fluorescein isothiocyanate (BD Biosciences, Franklin Lakes, NJ) and 5 μl propidium iodide (Sigma, St. Louis, MO) for 15 minutes in darkness. Degree of apoptosis was analyzed by fluorescence activated cell sorting. The proportion of stained cells in each quadrant was quantified with CellQuest software (BD Biosciences, Franklin Lakes, NJ). Experiments were performed in triplicate.

Invasion Assay

For assessment of invasion capability, invasion assay was performed using cell invasion assay kit system: Boyden chamber assay (8-μm pore sizes, 24-well)(Merck Millipore, Billerica, MA). Confluent Huh-BAT AR and HepG2 AR cells were seeded in serum-free DMEM at a density of 10^5 cells/upper chamber. Huh-BAT AR and HepG2 AR cells were treated as indicated (vehicle control, 200 μM of BSO, 40 μM of 3-BP, or a combination treatment of 3-BP and BSO). Chambers were installed in DMEM containing 10% FBS. Cells were incubated at 24-well plate at 37℃, 5% CO2. After 24 hours, cells which had not moved to the lower wells were removed from the upper chamber using clean cotton swabs, and cells that had moved to the lower surface of the filter were stained by using a staining solution. Cell invasion was quantified by visual counting after being photographed. Experiments were performed in triplicate. Mean values for three random fields were obtained for each well.

HCC Xenograft Mouse Models

Five-week-old male BALB/c nude mice were purchased from Orient Bio (Gyeonggi-do,

Korea). To generate tumors, Huh-BAT and Huh-BAT AR cells were subcutaneously inoculated with 1×10^7 cells at the right flank. After solid tumor formation (i.e., tumor volume 100 mm^3), all mice bearing Huh-BAT AR cells were divided into 4 groups randomly, and each group consisted of 10 mice: (i) control (vehicle alone), (ii) sorafenib (once a day intraperitoneal injection of 1.25 mg/kg for 2 weeks), (iii) 3-BP (once a day intraperitoneal injection of 1.8 mg/kg for 2 weeks), and (iv) a combination treatment of 3-BP (twice treatments one day and then rest one day regimen repeatedly for 2 weeks with intraperitoneal injection of 1.8 mg/kg) and BSO (every other day intraperitoneal injection of 250 mg/kg for 2 weeks)

The body weights of mouse were measured every other day with electronic scale. Tumor size was measured every other day with electronic caliper and the volume was calculated by the following formula: tumor volume = (length × width × height) /2 (60, 61). After finishing the treatment schedule, mice were anesthetized with isoflurane and tissue, tumors were harvested for analysis. All the protocols for the animal experiments were reviewed and approved by the Institutional Animal Care and Use Committee at Seoul National University Hospital (IACUC No. 14-0207-S1A1). All animal procedures were in consistent with the "Guide for the Care and Use of Laboratory Animals" issued by the Institute of Laboratory Animal Resources Commission on Life Science, US National Research Council.

Statistical Analysis

All experimental results represent at least 3 independent experiments using cells from a minimum of three separate isolations. Data were expressed as means ± SEM. P values were calculated with Student's paired *t* tests, or repeated measures ANOVA (SPSS, version 19.0, SPSS, Inc., Chicago, IL, USA). $P<0.05$ was considered statistically significant.

Results

Induction of Glycolysis and Antioxidant Systems by Matrix Detachment in HCC AR Cells

The morphology of HCC AR and HCC attached cells was different. Huh-BAT AR and HepG2 AR cells were round and clustered (Fig. 1A and 1B); Huh-BAT and HepG2 cells were polygonal and scattered (Fig. 1C and 1D). Huh-BAT AR and HepG2 AR cells upregulated HK II, p-PDH, and rGCS enzyme as compared to Huh-BAT and HepG2 cells (Fig. 2). Expression of HK II and rGCS was increased for 24 and 6 hours in Huh-BAT AR and HepG2 AR cells, respectively; expression of rGCS was induced more rapidly than HK II expression following cell detachment. These observations demonstrate that human HCC AR cells increase expression of enzymes involved in glycolysis and antioxidant system in response to matrix detachment. Expression of E-cadherin and Snail was changed 2 hours after matrix detachment in Huh-BAT and HepG2 AR cells: E-cadherin expression was decreased and Snail expression increased in Huh-BAT AR and HepG2 AR cells as compared to Huh-BAT (Fig. 3A) and HepG2 cells (Fig. 3B).

Intracellular lactic acid levels, the end-product of glycolysis, in Huh-BAT AR and HepG2 AR cells were significantly increased than those in Huh-BAT and HepG2 cells ($P<0.001$ in Huh-BAT AR cells; $P<0.001$ in HepG2 AR cells)(Fig. 4A). Intracellular ROS levels, which reflect intracellular redox status in Huh-BAT AR and HepG2 AR cells, were significantly decreased than Huh-BAT and HepG2 cells ($P=0.039$ in Huh-BAT AR cells; $P=0.021$ in HepG2 AR cells)(Fig. 4B).

Chemoresistance and Tumor Growth Rates in HCC AR Cells

Huh-BAT AR and HepG2 AR cells showed significantly higher viabilities at each concentration of sorafenib, doxorubicin, 5-fluorouracil (5-FU), and cisplatin than Huh-BAT and HepG2 cells; Huh-BAT AR and HepG2 AR cells showed chemoresistance ($P=0.021$,

sorafenib; P=0.002, 5-FU; P=0.036, cisplatin in Huh-BAT AR cells and P=0.002, sorafenib; P=0.022, 5-FU in HepG2 AR cells)(Fig. 5A and 5B).

After sorafenib treatment, viabilities of Huh-BAT AR and HepG2 AR cells were differed from those of Huh-BAT and HepG2 cells. At high dose of sorafenib 5 and 10 μM, Huh-BAT AR and HepG2 AR cells showed significantly higher viabilities than Huh-BAT and HepG2 cells (P=0.003 at sorafenib 5 μM; P=0.001 at sorafenib 10 μM in Huh-BAT AR cells and P=0.016 at sorafenib 5 μM; P=0.029 at sorafenib 10 μM in HepG2 AR cells)(Fig. 5C and 5D).

When tumor growth rates of Huh-BAT AR cells were compared to those of Huh-BAT cells, tumors derived from Huh-BAT AR cells in a mouse xenograft model grew significantly faster than those from Huh-BAT cells (P=0.026)(Fig. 6).

Intracellular ROS Levels Increased by 3-BP, BSO, and a Combination Treatment of 3-BP and BSO

In Huh-BAT AR and HepG2 AR cells treated with BSO (200 μM) for 24 hours, expression of rGCS enzyme was potentiated (Fig. 7A). A combination treatment of 3-BP and BSO in Huh-BAT AR and HepG2 AR cells induced rGCS expression via negative feedback to adjust for increased ROS levels (Fig. 7B).

BSO (200 μM) treatment and a combination treatment of 3-BP (40 μM) with BSO (200 μM) significantly suppressed intracellular GSH production (P<0.001, BSO; P<0.001, a combination treatment of 3-BP and BSO in Huh-BAT AR cells and P=0.001, BSO; P=0.001, a combination treatment of 3-BP and BSO in HepG2 AR cells)(Fig. 8). Intracellular ROS production in Huh-BAT AR (Fig. 9A) and HepG2 AR cells (Fig. 9B) was significantly increased after 3-BP (40 μM), BSO (200 μM), and a combination treatment of 3-BP and BSO as compared to the control (P=0.003, 3-BP; P=0.02, BSO; P=0.002, a combination treatment of 3-BP and BSO in Huh-BAT AR cells and P<0.001, 3-BP; P=0.008, BSO; P=0.003, a combination treatment of 3-BP

and BSO in HepG2 AR cells)(Fig. 9C).

Modulation of Glycolysis by 3-BP, BSO, and a Combination Treatment of 3-BP and BSO

Expression of HK II was suppressed 2 hours after 3-BP (40 μM) treatment in Huh-BAT, HepG2, and corresponding AR cells (Fig. 7A). 3-BP treatment significantly suppressed lactic acid production in those cells as compared to the control (P=0.038 in Huh-BAT; P<0.001 in Huh-BAT AR; P<0.001 in HepG2; P=0.002 in HepG2 AR cells)(Fig. 10A).

Expression of HK II was increased when Huh-BAT, HepG2, and corresponding AR cells were treated with BSO (Fig. 7A). Lactic acid production in Huh-BAT, HepG2 cells, and corresponding AR cells was significantly increased 48 hours after BSO (200 μM) treatment (P<0.001 for Huh-BAT; P<0.002 for Huh-BAT AR; P<0.001 for HepG2; P<0.001 for HepG2 AR cells)(Fig. 10B). A combination treatment of 3-BP (40 μM) and BSO (200 μM) significantly suppressed lactic acid production in Huh-BAT AR and HepG2 AR cells as compared to the control: 12 hours after 3-BP (40 μM) treatment on HCC AR cells pre-exposed to BSO (200 μM) treatment for 24 hours (P<0.001 in Huh-BAT AR; P=0.01 in HepG2 AR cells)(Fig. 10C). A combination treatment of 3-BP (40 μM) and BSO (200 μM) suppressed HK II expression in Huh-BAT AR and HepG2 AR cells (Fig. 7B).

Synergistic Anti-tumor Effects of a Combination Treatment of 3-BP and BSO in HCC AR Cells

In Huh-BAT and Huh-BAT AR cells, 3-BP effectively inhibited tumor growth at the concentration higher than 40 μM in 48 hours exposure (Fig. 11A). When treated with 3-BP, viabilities of Huh-BAT AR cells were not significantly different from those of Huh-BAT cells. After BSO treatment, viabilities of Huh-BAT AR cells at each concentration were significantly suppressed than those of Huh-BAT cells (all, P<0.05)(Fig. 11B). Cytotoxicity of BSO did not

show dose-dependent manner in Huh-BAT and Huh-BAT AR cells.

In HepG2 and HepG2 AR cells, at concentrations higher than 10 μM of 3-BP, HepG2 AR cells showed significant higher viabilities as compared to HepG2 cells (all, $P<0.01$)(Fig. 11C). When those cells were treated with 200 or 400 μM of BSO, there were no significant differences between HepG2 and HepG2 AR cells (Fig. 11D). At the highest concentration of 800 μM, viabilities of HepG2 AR cells were significantly lower than those of HepG2 cells ($P=0.04$)(Fig. 11D).

When HCC attached and AR cells were treated with a combination treatment of 3-BP and BSO, cell viabilities were effectively suppressed at 3-BP concentrations higher than 40 μM with pre-treatment of BSO (200 μM). There was no significant difference of cell viabilities between HCC attached and AR cells: Huh-BAT AR (Fig. 12A) and HepG2 AR cells (Fig. 12B).

A combination treatment of 3-BP and BSO increased apoptosis rates of Huh-BAT, HepG2, and corresponding AR cells as compared to the control ($P=0.026$ in Huh-BAT; $P=0.001$ in Huh-BAT AR; $P=0.004$ in HepG2; $P=0.002$ in HepG2 AR cells)(Fig. 13). When compared to the apoptosis rates in each treatment of 3-BP or BSO, a combination treatment of 3-BP and BSO showed higher apoptosis rates in Huh-BAT, HepG2, and corresponding AR cells ($P=0.012$, 3-BP in Huh-BAT cells; $P=0.002$, BSO and $P=0.001$, 3-BP in Huh-BAT AR cells; $P=0.001$, BSO and $P=0.002$, 3-BP in HepG2 cells; $P=0.002$, BSO and $P=0.001$, 3-BP in HepG2 AR cells).

Suppression of HCC Invasion by a Combination Treatment of 3-BP and BSO

As shown in Fig. 14A and 14C, 3-BP (40 μM), BSO (200 μM), and the combined 3-BP (40μM) with BSO (200 μM) treatment in Huh-BAT AR and HepG2 AR cells significantly suppressed cell invasion as compared with the control ($P=0.002$, 3-BP; $P=0.001$, BSO; $P=0.001$, a combination treatment of 3-BP and BSO in Huh-BAT AR cells and $P=0.006$, 3-BP; $P<0.001$, BSO; $P<0.001$, a combination treatment of 3-BP and BSO in HepG2 AR cells)(Fig. 14B and

14C). A combination treatment of 3-BP and BSO showed significantly higher suppression of cell invasion as compared with 3-BP alone in Huh-BAT AR cells; BSO and 3-BP alone in HepG2 AR cells (P=0.026, 3-BP, in Huh-BAT AR cells; P=0.008, 3-BP and P=0.019, BSO in HepG2 AR cells)(Fig. 14B and 14C).

Anti-tumor Effects of a Combination Treatment of 3-BP and BSO in Xenograft HCC AR Models

In the xenograft mouse model of Huh-BAT AR cells, there were four groups such as the control group (vehicle), the group for 3-BP treatment alone, the group for sorafenib treatment alone, and the group for a combination treatment of 3-BP and BSO. Tumor buds were grown 10–12 days after implantation of Huh-BAT AR cells on the back of each mouse.

There was no significant difference of growth rates of tumor volume between the control group and the group for 3-BP or sorafenib treatment alone (P=0.437 for sorafenib alone; P=0.243 for 3-BP alone)(Fig. 15A). However, the group for 3-BP or sorafenib treatment alone showed tendency to lower tumor growth rates as compared to the control group. There was no significant difference of tumor growth rates between 3-BP and sorafenib treatment alone (P=0.092). During each treatment, tumor growth rates in the group for a combination treatment of 3-BP and BSO were significantly lower than those in the group for control, sorafenib, and 3-BP treatment alone (P=0.008, P=0.011, and P=0.013, respectively)(Fig. 15A).

To quantify apoptosis of tumors, TUNEL staining was performed. Apoptosis index was significantly higher in the group for a combination treatment of 3-BP and BSO as compared to other groups (P<0.001, control; P=0.001, the sorafenib treatment group; P=0.004, the 3-BP treatment group)(Fig. 15B and 15C). The percentage of TUNEL-stained cells in the group for 3-BP or sorafenib treatment alone was not significantly different from that in the control

group (P=0.140 for 3-BP: P=0.262 for sorafenib). There was a significant difference of body weight between the control group and a combination treatment group (P=0.021)(Fig. 15D).

Discussion

Five important findings emerged from this study: 1) expression of key enzymes involved in glycolysis, antioxidant system, and EMT process such as HK II, p-PDH, rGCS, E-cadherin, and Snail was upregulated upon matrix detachment; 2) as compared to HCC attached cells, HCC AR cells significantly increased lactic acid production and decreased ROS generation; 3) HCC AR cells showed characteristics of chemoresistance for conventional chemotherapy agents, particularly sorafenib, and higher tumor growth rates than HCC attached cells in animals; 4) high intracellular ROS levels accelerated glycolysis rates via HK II induction; 5) a combination treatment of 3-BP and BSO effectively showed suppression of HCC AR and attached cells proliferation rates through apoptosis, and inhibited tumor growth as compared to 3-BP or sorafenib treatment alone in a xenograft mouse model bearing HCC AR cells.

Many earlier studies had shown that the Warburg effect, i.e., high glycolysis rates in presence of oxygen plays a key role to diminish glucose oxidation, promotes anoikis resistance and metastasis in cancer cells (14). ROS can be produced in mitochondria during aerobic metabolism due to dysregulated electron transport. However, under detached status, i.e., anoikis resistance which had been known as the first step for metastasis, HCC cells attenuate glucose oxidative metabolism to reduce the associated generation of ROS (14). The Warburg metabolic phenotype allows cancer cells to evade excessive ROS levels generated by mitochondrial respiration, and thereby cancer cells acquire a survival advantage when detached contributing to anoikis resistance (14).

In response to matrix detachment, cancer cells activate at least two programs such as ROS-scavenging system and glycolysis to counter cellular oxidative stress after detachment and thus delay anoikis. Given possible underlying mechanisms of the Warburg effect and ROS vulnerability in detached status (62, 63), a combination treatment to pharmacologically target cell's capacity of ROS detoxification and inhibit glycolysis may maximally provoke oxidative

stress and deplete ATP levels in cancer cells, which may represent an effective strategy to lower the threshold for apoptosis, restore anoikis sensitivity, and reduce metastasis and chemoresistance.

These features have a clinical significance in HCC treatment because characteristics of high glycolysis rates and antioxidant system in HCC AR cells were similar to those in cancer stem cells (CSCs). Two characteristics of high lactic acid production and low ROS levels were important to maintain a subpopulation of CSCs within some cancer types (64). Previous studies showed that glucose plays a major role in promoting CSC phenotype through the AMPK pathway, and that CSCs were more glycolytic as compared to the more differentiated cancer cells (64, 65). The mechanism whereby ROS levels are kept low in CSCs appears to involve upregulation of ROS-scavenging molecules, thereby contributing to tumor chemoresistance and radio-resistance as compared to differentiated and proliferative cancer cell populations (66). CSCs in gastrointestinal tumors with high expression of CD44 showed an increased capacity of GSH synthesis and defense of ROS detoxification by a cysteine–glutamate exchange transporter (67). Previous studies also showed that increase of intracellular ROS levels is accompanied by a significantly reduced number of CD44 high, CD24 low, and EpCAM positive CSCs, and decreased sphere formation (68).

Although two characteristics were important phenomenon in CSCs, there were lack of studies for anticancer effects when both systems, i.e., glycolysis and antioxidant systems, are blocked, and how two systems interplay in HCC AR cells. In this study, potent anti-tumor effects of a combination treatment, potent glycolytic inhibitor of 3-BP with an ROS enhancer of BSO, were shown in HCC AR cells which can mimic CSCs' features. Furthermore, given a recent study indicated that non-stem cancer cells can also give rise to CSCs, suggesting the bi-directional transformation between these two populations (69), this was an important

finding that a combination treatment of 3-BP and BSO effectively suppressed HCC attached cell as well as HCC AR cells using close linking between glycolysis and ROS status.

Our results demonstrated that intracellular ROS levels modulated the Warburg effect in HCC AR cells. In other words, the Warburg effect and antioxidant system were not independent and parallel pathways in HCC AR cells: increased ROS levels after BSO treatment stimulated glycolytic pathway via HK II induction. It could be explained by that to evade excess ROS production in energy metabolism, the cancer cells pre-treated with BSO potentiated the Warburg effect, less dependent on mitochondrial oxidation, and could be more sensitive to 3-BP treatment as compared to those cells not pre-treated with BSO: flexibility of the Warburg effect (Fig. 15).

With focus on BSO effects on ROS levels, previous studies reported that increased ROS levels can facilitate tumor growth, invasion, and angiogenesis (70). A major implication of our findings is that antioxidants might not be beneficial in some cancer conditions such as a step for initiation of metastasis. Cancerous tissues were reported to produce increased amounts of ROS (71). Suboptimal levels of ROS below the toxic threshold stimulating apoptosis activate signaling pathways such as Src, PI3K, NF-kB, and HIF that may increase cell proliferation and survival under mild oxidative conditions, and contribute to cellular transformation (72). By contrast, high ROS levels above the toxic threshold required for signaling may cause strong oxidative damage that can result in senescence or death in both normal and cancer cells (63). Therefore, it would be important to delivery high dose of BSO or other ROS enhancers to amplify intracellular ROS levels sufficient to stimulate the apoptosis signals at the tumor site. Under physiological conditions, normal cells maintain redox homeostasis with a low level of baseline intracellular ROS levels by controlling the balance between ROS production and elimination. Normal cells can tolerate a certain level of

exogenous ROS stress due to their antioxidant capacity, which can be mobilized to maintain the ROS level far from the toxic threshold initiating apoptosis. However, cancer cells show a shift of redox dynamics with high ROS production and elimination to maintain the ROS levels below the toxic threshold (15, 63). In other words, there is not enough space between intracellular high ROS levels and the toxic threshold. Therefore, cancer cells would be more dependent on the antioxidant system and more vulnerable to further oxidative stress induced by exogenous ROS-generating agents that inhibit the antioxidant system (15, 63). Besides rGCS, other important cellular antioxidants such as MnSOD, thioredoxin, glutaredoxin, and peroxiredoxin are upregulated in some cancer cells (24). Pro-malignant potential of antioxidants has been increasingly recognized. This might constitute a biochemical basis to design therapeutic strategies to selectively kill cancer cells using ROS-mediated mechanisms. In addition, this antioxidant system is related to chemoresistance. Common cancer therapies may kill cancer cells by promoting oxidative stress (63). To cope with high oxidative stress induced by chemotherapy, cancer cells develop chemoresistance by potentiation of antioxidant systems. Taken together, it is important to delivery ROS amplifying agents specifically to a tumor target and effectively increase intracellular ROS levels enough to stimulate the apoptosis pathway. In previous reports, a potent ROS enhancer of piperlongumine exerted potent anticancer effects on HCC cells via ROS accumulation (73).

Both HCC AR and attached cells were sensitive to the combination treatment targeting the Warburg effects and antioxidant system: not targeting one side of AR or attached cells. The mechanism for synergistic effects of 3-BP after BSO treatment can be explained by ROS-mediated apoptosis and energy depletion. Cancer cells display high glycolytic flux through glycolysis and other metabolic pathways originating from glycolytic intermediates. These metabolic pathways are involved in the synthesis of essential amino acids, lipids and nucleotides through pentose phosphate shunt. 3-BP can target rapid proliferative cells by

blocking glycolytic flux which may be essential for high demand for cellular macromolecules: suppression of highly adaptive energy production (74). In addition to energy block by 3-BP, each compound of BSO and 3-BP significantly increased ROS levels. This can target HCC cells which were vulnerable to ROS stress. Given that suspended status itself can normally stimulate intracellular ROS production, HCC AR cells can be more vulnerable to excess of ROS oxidative stress enhanced by 3-BP or BSO treatment. In addition to BSO effects on oxidative stress above the toxic threshold, BSO also sensitized cancer cells to 3-BP treatment by increasing glycolysis through HK II induction.

In real practical field, most of HCCs recur as multinodular pattern and/or portal vein invasion although single HCC at the first presentation was successfully removed. Early recurrence with multinodular pattern and/or portal vein invasion after resection of HCCs occurs due to microvascular invasion/micro-metastasis of HCC into normal liver parenchyma. Current guidelines recommend optimal treatments such as trans-arterial chemoembolization for patients with multinodular HCCs without portal vein invasion and sorafenib treatment for patients with multinodular HCC with portal vein invasion. However, survival benefits were not satisfactory. Furthermore, there have been no clinical trials suggesting survival benefits of adjuvant chemotherapy after curative resection of HCC in Barcelona clinic liver cancer stage 0 or A. This study has a clinical implication to suggest an alternative for patients who showed poor response to trans-arterial chemoembolization such as refractoriness and sorafenib treatment. Because a combination treatment of 3-BP and BSO can target both types of HCC attached and AR cells, there are high possibilities that a combination treatment of 3-BP and BSO can suppress HCC recurrences, microvascular invasion, and portal vein invasion.

However, this study had some limitations. First, BSO treatment could not specifically target cancer cells. In other words, BSO treatment can injury normal cells by increasing intracellular ROS levels. Given that ROS homeostasis is important for cell senescence, renewal, and inflammation, adverse effects of increased oxidative stress by BSO treatment should be considered. Particularly, in this study, body weights of mouse treated by a combination of 3-BP and BSO were significantly decreased as compared to those treated by single treatment or the control group: it reflects toxicity of potentiated oxidative stress by a combination treatment of 3-BP and BSO. Therefore, to minimize toxicity of nonspecific ROS enhancers such as BSO, it should be clarified how ROS enhancers can be specifically delivered to the tumor sites, and what compounds/ molecules can effectively maximize oxidative stress only in cancer cells. Given that previous studies suggested the safety and specificity of 3-BP to target cancer cells in animal models, the safety and nonspecific targeting problems in BSO treatment should be elucidated before we move forward to the clinical field using a combination treatment of 3-BP and BSO. Second, in this study, there was a lack of animal data suggesting that tumors originated from HCC AR cells more aggressively metastasized to distant organs as compared to those from HCC attached cells. Although results in this study showed that tumors induced from HCC AR cells had grown more rapidly than those from HCC attached cells, it might be difficult to prove that capability of metastasis in tumors derived from HCC AR cells was significantly higher than that in those from HCC attached cells. Further studies using animal metastasis models might be needed to clarify this difference of metastasis capability between tumors from HCC AR cells and those from HCC attached cells.

In conclusion, human HCC AR cells showed similar characteristics of CSCs such as chemoresistance, particularly sorafenib resistance, aggressive growth phenotype, higher glycolysis, metastatic potential, and antioxidant systems as compared to HCC attached cells.

A combination treatment targeting glycolysis and antioxidant systems effectively suppressed HCC AR and attached cell growth. Given anti-tumor effects of sorafenib can be modest when HCC patients have a large burden of tumor such as intrahepatic or extrahepatic metastasis of HCC (75), this option suggests alternative therapy for HCC patients with intrahepatic and/or extrahepatic metastasis who show poor response to sorafenib treatment.

References

1. Jemal A, Bray F, Center MM, Ferlay J, Ward E, Forman D. Global cancer statistics. CA: a cancer journal for clinicians. 2011;61(2):69-90.

2. de Lope CR, Tremosini S, Forner A, Reig M, Bruix J. Management of HCC. Journal of hepatology. 2012;56 Suppl 1:S75-87.

3. Earl TM, Chapman WC. Hepatocellular carcinoma: resection versus transplantation. Seminars in liver disease. 2013;33(3):282-92.

4. Llovet JM, Schwartz M, Mazzaferro V. Resection and liver transplantation for hepatocellular carcinoma. Seminars in liver disease. 2005;25(2):181-200.

5. Kumada T, Nakano S, Takeda I, Sugiyama K, Osada T, Kiriyama S, et al. Patterns of recurrence after initial treatment in patients with small hepatocellular carcinoma. Hepatology. 1997;25(1):87-92.

6. Llovet JM, Ricci S, Mazzaferro V, Hilgard P, Gane E, Blanc JF, et al. Sorafenib in advanced hepatocellular carcinoma. The New England journal of medicine. 2008;359(4):378-90.

7. Chan SL, Yeo W. Development of systemic therapy for hepatocellular carcinoma at 2013: updates and insights. World journal of gastroenterology : WJG. 2014;20(12):3135-45.

8. Taddei ML, Giannoni E, Fiaschi T, Chiarugi P. Anoikis: an emerging hallmark in health and diseases. The Journal of pathology. 2012;226(2):380-93.

9. Simpson CD, Anyiwe K, Schimmer AD. Anoikis resistance and tumor metastasis. Cancer letters. 2008;272(2):177-85.

10. Strauss SJ, Ng T, Mendoza-Naranjo A, Whelan J, Sorensen PH. Understanding micrometastatic disease and Anoikis resistance in ewing family of tumors and osteosarcoma. The oncologist. 2010;15(6):627-35.

11. Mehlen P, Puisieux A. Metastasis: a question of life or death. Nature reviews Cancer. 2006;6(6):449-58.

12. Schmidt M, Hovelmann S, Beckers TL. A novel form of constitutively active farnesylated Akt1 prevents mammary epithelial cells from anoikis and suppresses chemotherapy-induced apoptosis. British journal of cancer. 2002;87(8):924-32.

13. Duxbury MS, Ito H, Benoit E, Waseem T, Ashley SW, Whang EE. A novel role for carcinoembryonic antigen-related cell adhesion molecule 6 as a determinant of gemcitabine chemoresistance in pancreatic adenocarcinoma cells. Cancer research. 2004;64(11):3987-93.

14. Kamarajugadda S, Stemboroski L, Cai Q, Simpson NE, Nayak S, Tan M, et al. Glucose oxidation modulates anoikis and tumor metastasis. Molecular and cellular biology. 2012;32(10):1893-907.

15. Cairns RA, Harris IS, Mak TW. Regulation of cancer cell metabolism. Nature reviews Cancer. 2011;11(2):85-95.

16. Anastasiou D, Poulogiannis G, Asara JM, Boxer MB, Jiang JK, Shen M, et al. Inhibition of pyruvate kinase M2 by reactive oxygen species contributes to cellular antioxidant responses. Science. 2011;334(6060):1278-83.

17. Lu CW, Lin SC, Chien CW, Lin SC, Lee CT, Lin BW, et al. Overexpression of pyruvate dehydrogenase kinase 3 increases drug resistance and early recurrence in colon cancer. The American journal of pathology. 2011;179(3):1405-14.

18. Wigfield SM, Winter SC, Giatromanolaki A, Taylor J, Koukourakis ML, Harris AL. PDK-1 regulates lactate production in hypoxia and is associated with poor prognosis in head and neck squamous cancer. British journal of cancer. 2008;98(12):1975-84.

19. Brand KA, Hermfisse U. Aerobic glycolysis by proliferating cells: a protective strategy against reactive oxygen species. FASEB journal : official publication of the Federation of

American Societies for Experimental Biology. 1997;11(5):388-95.

20. Kawanishi S, Hiraku Y, Pinlaor S, Ma N. Oxidative and nitrative DNA damage in animals and patients with inflammatory diseases in relation to inflammation-related carcinogenesis. Biological chemistry. 2006;387(4):365-72.

21. Szatrowski TP, Nathan CF. Production of large amounts of hydrogen peroxide by human tumor cells. Cancer research. 1991;51(3):794-8.

22. Sayin VI, Ibrahim MX, Larsson E, Nilsson JA, Lindahl P, Bergo MO. Antioxidants accelerate lung cancer progression in mice. Science translational medicine. 2014;6(221):221ra15.

23. Kamarajugadda S, Cai Q, Chen H, Nayak S, Zhu J, He M, et al. Manganese superoxide dismutase promotes anoikis resistance and tumor metastasis. Cell death & disease. 2013;4:e504.

24. Landriscina M, Maddalena F, Laudiero G, Esposito F. Adaptation to oxidative stress, chemoresistance, and cell survival. Antioxidants & redox signaling. 2009;11(11):2701-16.

25. Pani G, Colavitti R, Bedogni B, Fusco S, Ferraro D, Borrello S, et al. Mitochondrial superoxide dismutase: a promising target for new anticancer therapies. Current medicinal chemistry. 2004;11(10):1299-308.

26. Toyokuni S. Novel aspects of oxidative stress-associated carcinogenesis. Antioxidants & redox signaling. 2006;8(7-8):1373-7.

27. Schumacker PT. Reactive oxygen species in cancer cells: live by the sword, die by the sword. Cancer cell. 2006;10(3):175-6.

28. Bey EA, Bentle MS, Reinicke KE, Dong Y, Yang CR, Girard L, et al. An NQO1- and PARP-1-mediated cell death pathway induced in non-small-cell lung cancer cells by beta-lapachone. Proceedings of the National Academy of Sciences of the United States of America. 2007;104(28):11832-7.

29. Alexandre J, Batteux F, Nicco C, Chereau C, Laurent A, Guillevin L, et al. Accumulation of hydrogen peroxide is an early and crucial step for paclitaxel-induced cancer cell death both in vitro and in vivo. International journal of cancer Journal international du cancer. 2006;119(1):41-8.

30. Trachootham D, Zhou Y, Zhang H, Demizu Y, Chen Z, Pelicano H, et al. Selective killing of oncogenically transformed cells through a ROS-mediated mechanism by beta-phenylethyl isothiocyanate. Cancer cell. 2006;10(3):241-52.

31. Fruehauf JP, Meyskens FL, Jr. Reactive oxygen species: a breath of life or death? Clinical cancer research : an official journal of the American Association for Cancer Research. 2007;13(3):789-94.

32. Ganapathy-Kanniappan S, Kunjithapatham R, Torbenson MS, Rao PP, Carson KA, Buijs M, et al. Human hepatocellular carcinoma in a mouse model: assessment of tumor response to percutaneous ablation by using glyceraldehyde-3-phosphate dehydrogenase antagonists. Radiology. 2012;262(3):834-45.

33. Yu SJ, Yoon JH, Yang JI, Cho EJ, Kwak MS, Jang ES, et al. Enhancement of hexokinase II inhibitor-induced apoptosis in hepatocellular carcinoma cells via augmenting ER stress and anti-angiogenesis by protein disulfide isomerase inhibition. Journal of bioenergetics and biomembranes. 2012;44(1):101-15.

34. Yu SJ, Yoon JH, Lee JH, Myung SJ, Jang ES, Kwak MS, et al. Inhibition of hypoxia-inducible carbonic anhydrase-IX enhances hexokinase II inhibitor-induced hepatocellular carcinoma cell apoptosis. Acta pharmacologica Sinica. 2011;32(7):912-20.

35. Ganapathy-Kanniappan S, Geschwind JF, Kunjithapatham R, Buijs M, Syed LH, Rao PP, et al. 3-Bromopyruvate induces endoplasmic reticulum stress, overcomes autophagy and causes apoptosis in human HCC cell lines. Anticancer research. 2010;30(3):923-35.

36. Kim JS, Ahn KJ, Kim JA, Kim HM, Lee JD, Lee JM, et al. Role of reactive oxygen species-mediated mitochondrial dysregulation in 3-bromopyruvate induced cell death in hepatoma cells : ROS-mediated cell death by 3-BrPA. Journal of bioenergetics and biomembranes. 2008;40(6):607-18.

37. Kim W, Yoon JH, Jeong JM, Cheon GJ, Lee TS, Yang JI, et al. Apoptosis-inducing antitumor efficacy of hexokinase II inhibitor in hepatocellular carcinoma. Molecular cancer therapeutics. 2007;6(9):2554-62.

38. Gwak GY, Yoon JH, Kim KM, Lee HS, Chung JW, Gores GJ. Hypoxia stimulates proliferation of human hepatoma cells through the induction of hexokinase II expression. Journal of hepatology. 2005;42(3):358-64.

39. Ko YH, Smith BL, Wang Y, Pomper MG, Rini DA, Torbenson MS, et al. Advanced cancers: eradication in all cases using 3-bromopyruvate therapy to deplete ATP. Biochemical and biophysical research communications. 2004;324(1):269-75.

40. Geschwind JF, Ko YH, Torbenson MS, Magee C, Pedersen PL. Novel therapy for liver cancer: direct intraarterial injection of a potent inhibitor of ATP production. Cancer research. 2002;62(14):3909-13.

41. Ko YH, Pedersen PL, Geschwind JF. Glucose catabolism in the rabbit VX2 tumor model for liver cancer: characterization and targeting hexokinase. Cancer letters. 2001;173(1):83-91.

42. Vali M, Liapi E, Kowalski J, Hong K, Khwaja A, Torbenson MS, et al. Intraarterial therapy with a new potent inhibitor of tumor metabolism (3-bromopyruvate): identification of therapeutic dose and method of injection in an animal model of liver cancer. Journal of vascular and interventional radiology : JVIR. 2007;18(1 Pt 1):95-101.

43. Yuan S, Wang F, Chen G, Zhang H, Feng L, Wang L, et al. Effective elimination of

cancer stem cells by a novel drug combination strategy. Stem cells. 2013;31(1):23-34.

44. Dai Y, Xiong X, Huang G, Liu J, Sheng S, Wang H, et al. Dichloroacetate enhances adriamycin-induced hepatoma cell toxicity in vitro and in vivo by increasing reactive oxygen species levels. PloS one. 2014;9(4):e92962.

45. Shen YC, Ou DL, Hsu C, Lin KL, Chang CY, Lin CY, et al. Activating oxidative phosphorylation by a pyruvate dehydrogenase kinase inhibitor overcomes sorafenib resistance of hepatocellular carcinoma. British journal of cancer. 2013;108(1):72-81.

46. Ricotti L, Tesei A, De Paola F, Milandri C, Amadori D, Frassineti GL, et al. Potentiation of antiproliferative drug activity by lonidamine in hepatocellular carcinoma cells. Journal of chemotherapy. 2003;15(5):480-7.

47. Wang CF, Wang YQ, Huang FZ, Nie WP, Liu XY, Jiang XZ. Association between reversal of multidrug resistance by methyl jasmonate and P-glycoprotein ATPase activity in hepatocellular carcinoma. The Journal of international medical research. 2013;41(4):964-74.

48. Park C, Jin CY, Hwang HJ, Kim GY, Jung JH, Kim WJ, et al. J7, a methyl jasmonate derivative, enhances TRAIL-mediated apoptosis through up-regulation of reactive oxygen species generation in human hepatoma HepG2 cells. Toxicology in vitro : an international journal published in association with BIBRA. 2012;26(1):86-93.

49. Park C, Jin CY, Kim GY, Cheong J, Jung JH, Yoo YH, et al. A methyl jasmonate derivative, J-7, induces apoptosis in human hepatocarcinoma Hep3B cells in vitro. Toxicology in vitro : an international journal published in association with BIBRA. 2010;24(7):1920-6.

50. Minchenko A, Leshchinsky I, Opentanova I, Sang N, Srinivas V, Armstead V, et al. Hypoxia-inducible factor-1-mediated expression of the 6-phosphofructo-2-kinase/fructose-2,6-bisphosphatase-3 (PFKFB3) gene. Its possible role in the Warburg effect. The Journal of biological chemistry. 2002;277(8):6183-7.

51. Pedersen PL. Warburg, me and Hexokinase 2: Multiple discoveries of key molecular events underlying one of cancers' most common phenotypes, the "Warburg Effect", i.e., elevated glycolysis in the presence of oxygen. Journal of bioenergetics and biomembranes. 2007;39(3):211-22.

52. Pedersen PL, Mathupala S, Rempel A, Geschwind JF, Ko YH. Mitochondrial bound type II hexokinase: a key player in the growth and survival of many cancers and an ideal prospect for therapeutic intervention. Biochimica et biophysica acta. 2002;1555(1-3):14-20.

53. Lee M, Yoon JH. Metabolic interplay between glycolysis and mitochondrial oxidation: The reverse Warburg effect and its therapeutic implication. World journal of biological chemistry. 2015;6(3):148-61.

54. Pedersen PL. 3-Bromopyruvate (3BP) a fast acting, promising, powerful, specific, and effective "small molecule" anti-cancer agent taken from labside to bedside: introduction to a special issue. Journal of bioenergetics and biomembranes. 2012;44(1):1-6.

55. Huang ZZ, Chen C, Zeng Z, Yang H, Oh J, Chen L, et al. Mechanism and significance of increased glutathione level in human hepatocellular carcinoma and liver regeneration. FASEB journal : official publication of the Federation of American Societies for Experimental Biology. 2001;15(1):19-21.

56. Backos DS, Franklin CC, Reigan P. The role of glutathione in brain tumor drug resistance. Biochemical pharmacology. 2012;83(8):1005-12.

57. Balendiran GK, Dabur R, Fraser D. The role of glutathione in cancer. Cell biochemistry and function. 2004;22(6):343-52.

58. Griffith OW, Mulcahy RT. The enzymes of glutathione synthesis: gamma-glutamylcysteine synthetase. Advances in enzymology and related areas of molecular biology. 1999;73:209-67, xii.

59. Armstrong JS, Steinauer KK, Hornung B, Irish JM, Lecane P, Birrell GW, et al. Role of glutathione depletion and reactive oxygen species generation in apoptotic signaling in a human B lymphoma cell line. Cell death and differentiation. 2002;9(3):252-63.

60. Reynolds CP, Sun BC, DeClerck YA, Moats RA. Assessing growth and response to therapy in murine tumor models. Methods in molecular medicine. 2005;111:335-50.

61. Tomayko MM, Reynolds CP. Determination of subcutaneous tumor size in athymic (nude) mice. Cancer chemotherapy and pharmacology. 1989;24(3):148-54.

62. Montero AJ, Jassem J. Cellular redox pathways as a therapeutic target in the treatment of cancer. Drugs. 2011;71(11):1385-96.

63. Trachootham D, Alexandre J, Huang P. Targeting cancer cells by ROS-mediated mechanisms: a radical therapeutic approach? Nature reviews Drug discovery. 2009;8(7):579-91.

64. Liu PP, Liao J, Tang ZJ, Wu WJ, Yang J, Zeng ZL, et al. Metabolic regulation of cancer cell side population by glucose through activation of the Akt pathway. Cell death and differentiation. 2014;21(1):124-35.

65. Ciavardelli D, Rossi C, Barcaroli D, Volpe S, Consalvo A, Zucchelli M, et al. Breast cancer stem cells rely on fermentative glycolysis and are sensitive to 2-deoxyglucose treatment. Cell death & disease. 2014;5:e1336.

66. Diehn M, Cho RW, Lobo NA, Kalisky T, Dorie MJ, Kulp AN, et al. Association of reactive oxygen species levels and radioresistance in cancer stem cells. Nature. 2009;458(7239):780-3.

67. Ishimoto T, Nagano O, Yae T, Tamada M, Motohara T, Oshima H, et al. CD44 variant regulates redox status in cancer cells by stabilizing the xCT subunit of system xc(-) and thereby promotes tumor growth. Cancer cell. 2011;19(3):387-400.

68. Dong C, Yuan T, Wu Y, Wang Y, Fan TW, Miriyala S, et al. Loss of FBP1 by Snail-mediated repression provides metabolic advantages in basal-like breast cancer. Cancer cell. 2013;23(3):316-31.

69. Chaffer CL, Brueckmann I, Scheel C, Kaestli AJ, Wiggins PA, Rodrigues LO, et al. Normal and neoplastic nonstem cells can spontaneously convert to a stem-like state. Proceedings of the National Academy of Sciences of the United States of America. 2011;108(19):7950-5.

70. Liou GY, Storz P. Reactive oxygen species in cancer. Free radical research. 2010;44(5):479-96.

71. Haklar G, Sayin-Ozveri E, Yuksel M, Aktan AO, Yalcin AS. Different kinds of reactive oxygen and nitrogen species were detected in colon and breast tumors. Cancer letters. 2001;165(2):219-24.

72. Gupta SC, Hevia D, Patchva S, Park B, Koh W, Aggarwal BB. Upsides and downsides of reactive oxygen species for cancer: the roles of reactive oxygen species in tumorigenesis, prevention, and therapy. Antioxidants & redox signaling. 2012;16(11):1295-322.

73. Chen Y, Liu JM, Xiong XX, Qiu XY, Pan F, Liu D, et al. Piperlongumine selectively kills hepatocellular carcinoma cells and preferentially inhibits their invasion via ROS-ER-MAPKs-CHOP. Oncotarget. 2015;6(8):6406-21.

74. Lunt SY, Vander Heiden MG. Aerobic glycolysis: meeting the metabolic requirements of cell proliferation. Annual review of cell and developmental biology. 2011;27:441-64.

75. Sohn W, Paik YH, Cho JY, Lim HY, Ahn JM, Sinn DH, et al. Sorafenib therapy for hepatocellular carcinoma with extrahepatic spread: treatment outcome and prognostic factors. Journal of hepatology. 2015;62(5):1112-21.

Figure Legends

Figure 1. Morphology of Huh-BAT, HepG2 cells, and corresponding HCC AR cells. Huh-BAT AR (A) and HepG2 AR cells (B) were clustered and showed round shapes in high power field (x 100 magnification). Huh-BAT (C) and HepG2 cells (D) showed polygonal shapes and grew under attached condition.

Abbreviation: AR, anoikis resistant.

(A)

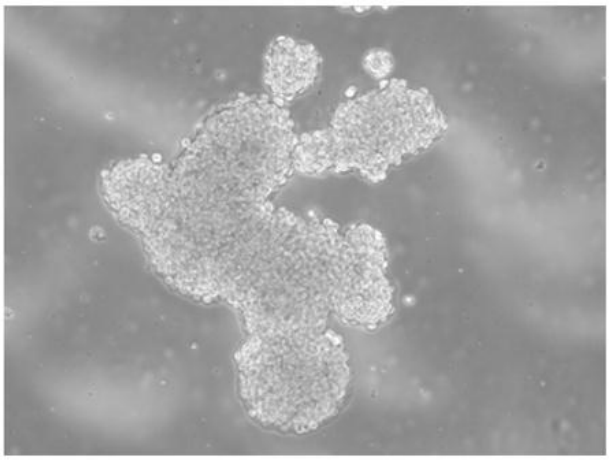

(B)

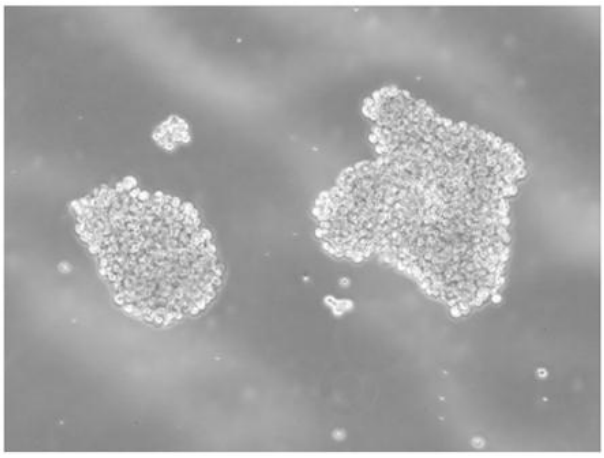

(C)

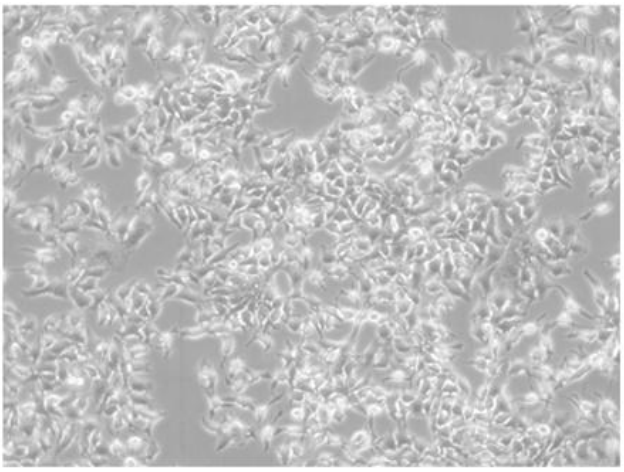

(D)

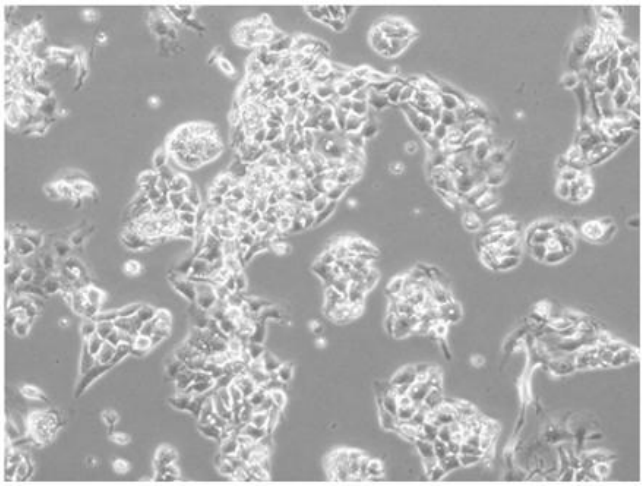

Figure 2. Induction of HK II, p-PDH, and rGCS expression in the HCC AR cells after matrix detachment. Huh-BAT AR (A) and HepG2 AR cells (B) showed higher expression of HK II, p-PDH, and rGCS as compared to Huh-BAT and HepG2 cells at the indicated time points after matrix detachment, respectively.

Abbreviation: Att, attached; AR, anoikis resistant; HK II, hexokinase II; hrs, hours; p-PDH, phosphorylated pyruvate dehydrogenase; rGCS, gamma-glutamylcysteine synthetase.

(A)

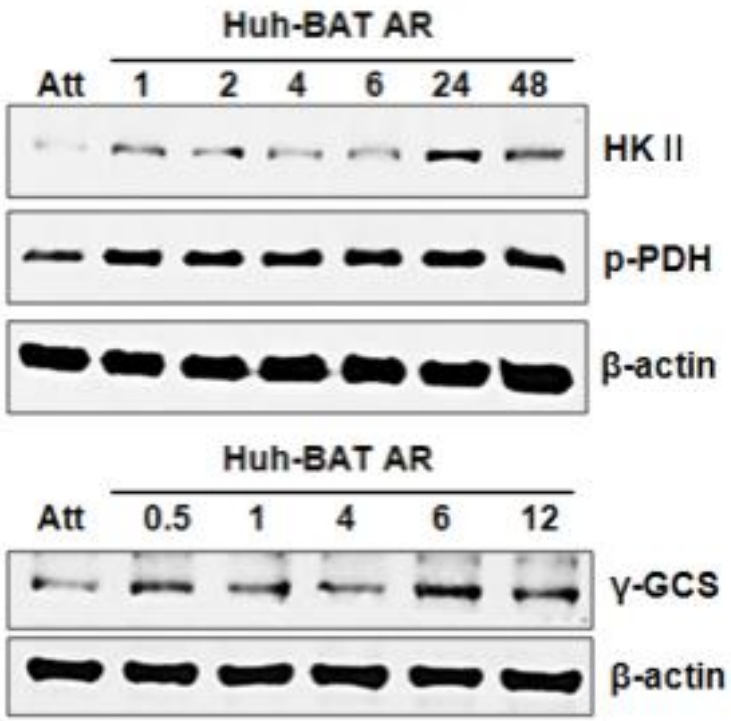

(B)

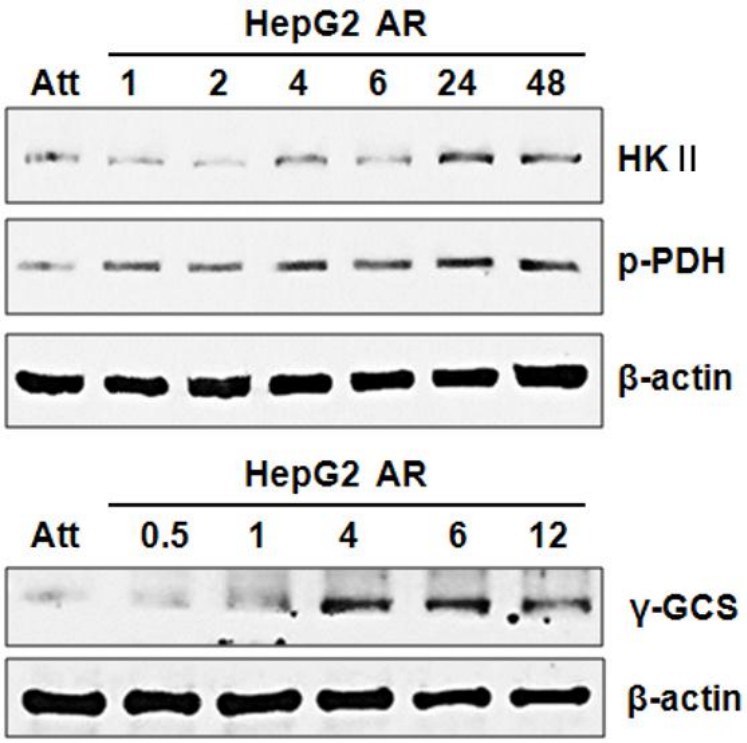
HepG2 AR
Att
1
2
4
6
24
48
HK II
p-PDH
β-actin
HepG2 AR
Att
0.5
1
4
6
12
γ-GCS
β-actin

Figure 3. Change of E-cadherin and Snail expression. Expression of E-cadherin 2 hours after matrix detachment was suppressed in Huh-BAT AR (A) and HepG2 AR (B) cells as compared to Huh-BAT and HepG2 cells, respectively: expression of Snail was potentiated in Huh-BAT AR (A) and HepG2 AR (B) cells as compared to Huh-BAT and HepG2 cells, respectively. Abbreviation: AR, anoikis resistant; Att, attached.

(A)

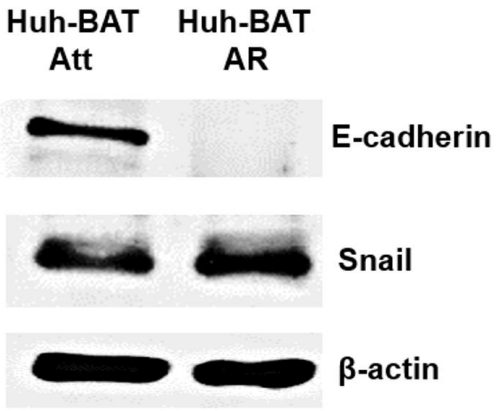

(B)

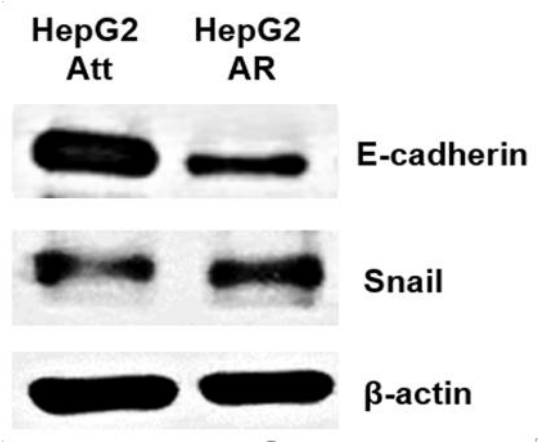

Figure 4. Change of intracellular lactic acid and ROS production after matrix detachment. (A) Lactic acid production in Huh-BAT AR and HepG2 AR cells was significantly increased than that in Huh-BAT and HepG2 cells: P<0.001 for Huh-BAT AR cell and P<0.001 for HepG2 AR cell. (B) ROS production in Huh-BAT AR and HepG2 AR cells was significantly decreased than that in Huh-BAT and HepG2 cells: P=0.039 for Huh-BAT AR cells and P=0.021 for HepG2 AR cells.

* means P<0.05; *** means P<0.001.

Abbreviation: AR, anoikis resistant; ROS, reactive oxygen species.

Bars, SD.

(A)

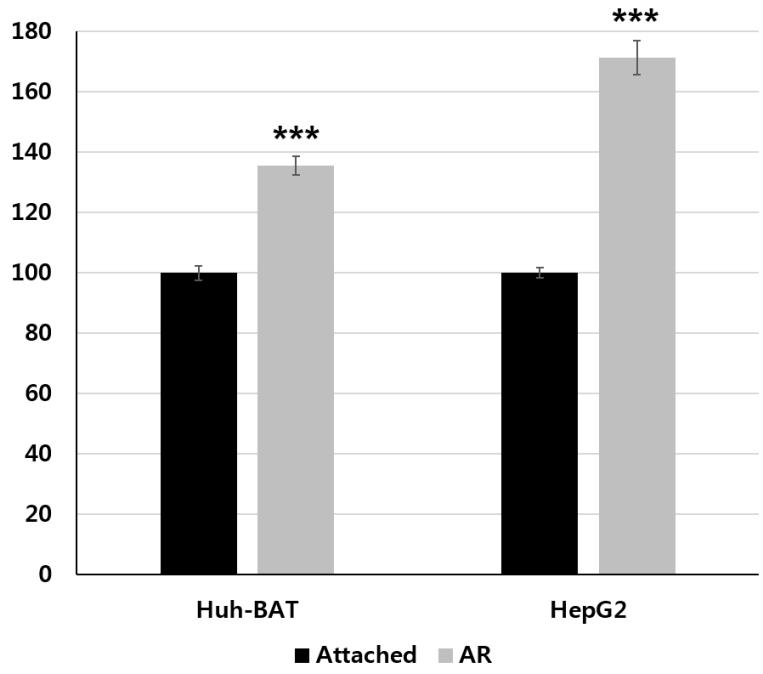

(B)

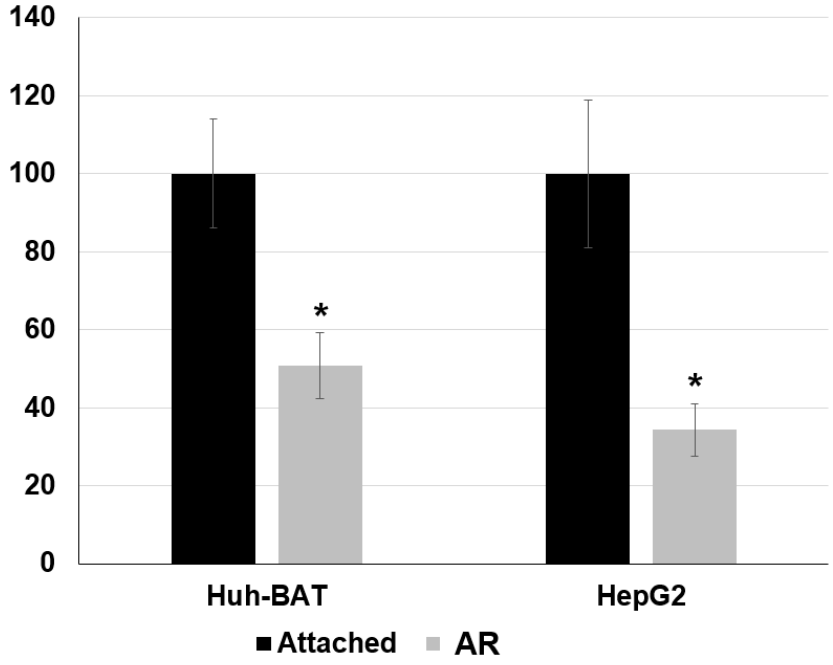

Figure 5. Chemoresistance phenotype of the HCC AR cells as compared to HCC attached cells. (A) Huh-BAT AR cells showed significantly higher viabilities at 3 μM of sorafenib, 1 μM of 5-FU, and 10 μM of cisplatin as compared to Huh-BAT cells. (B) HepG2 AR cells showed significantly higher viabilities at 3 μM of sorafenib and 1 μM of 5-FU as compared to HepG2 cells. (C) Huh-BAT AR and (D) HepG2 AR cells showed significantly higher viabilities at concentration of 5 and 10 μM of sorafenib as compared to Huh-BAT and HepG2 cells.

* means $P<0.05$; ** means $P<0.01$.

Abbreviation: AR, anoikis resistant; sora, sorafenib; 5-FU, 5-fluorouracil.

Bars, SD.

(A)

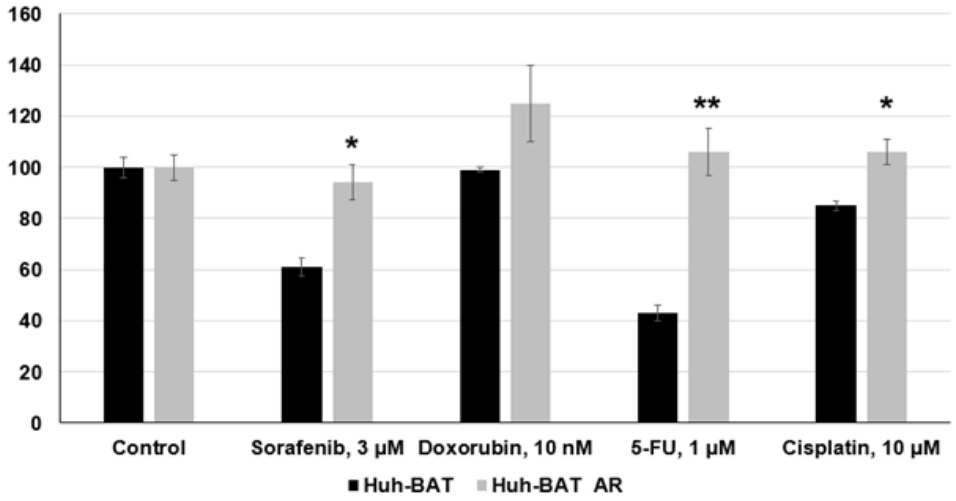

(B)

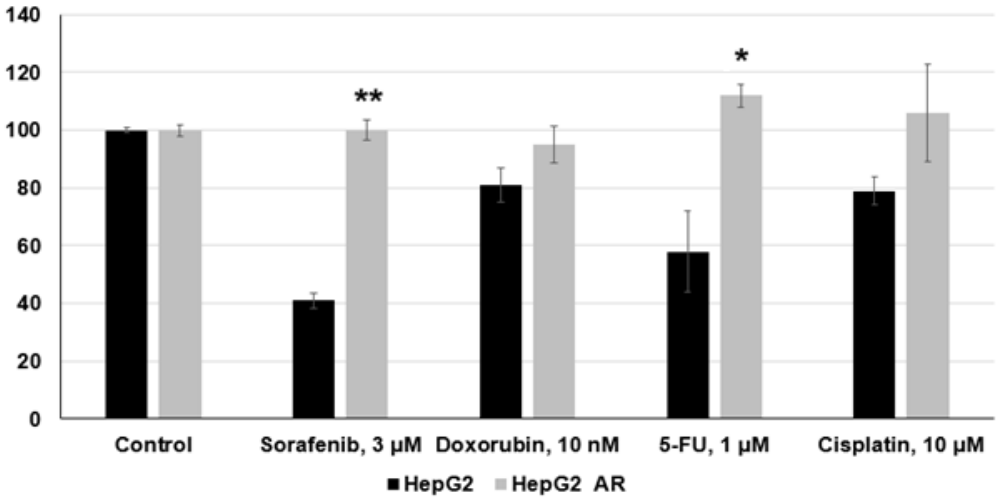
140
120
100
80
60
40
20
0
**
*
Control
Sorafenib, 3 μM
Doxorubin, 10 nM
5-FU, 1 μM
Cisplatin, 10 μM
HepG2
HepG2 AR

(C)

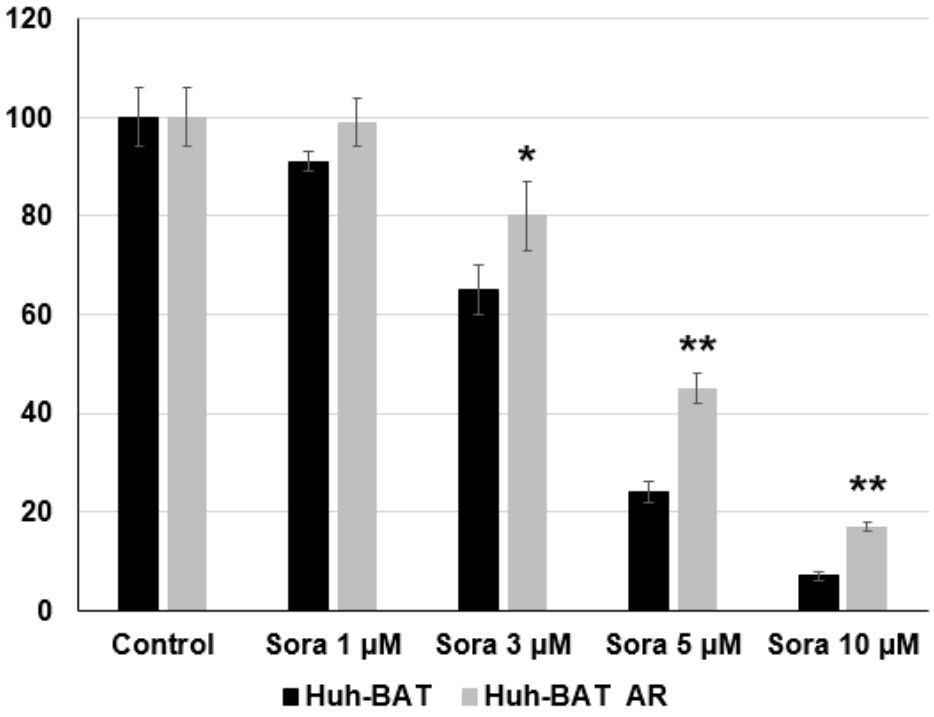
120
100
80
60
40
20
0
*
**
**
Control
Sora 1 μM
Sora 3 μM
Sora 5 μM
Sora 10 μM
Huh-BAT
Huh-BAT AR

(D)

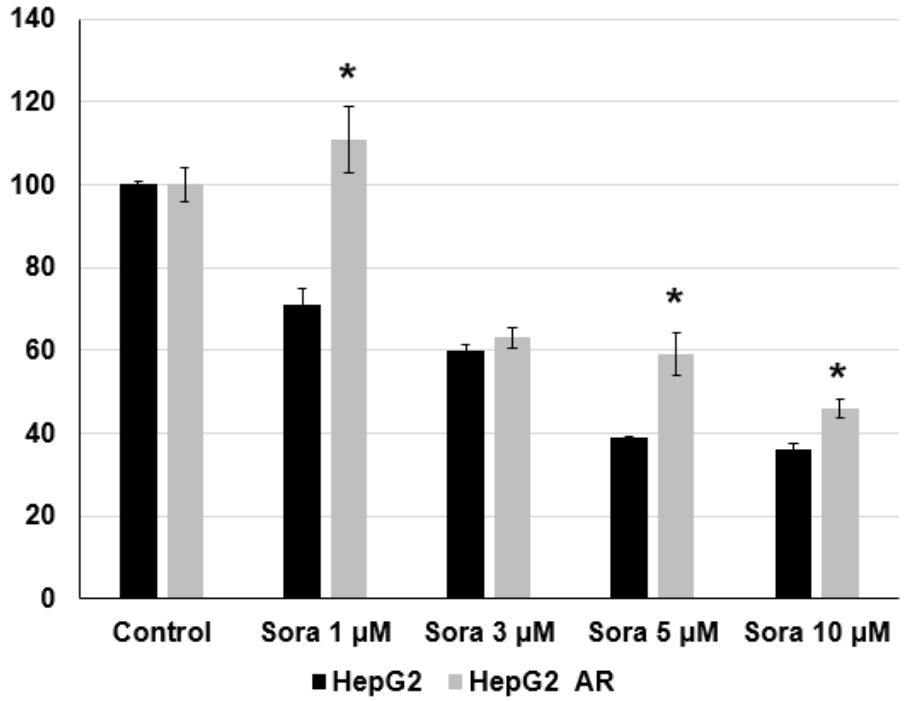
140
120
100
80
60
40
20
0
*
*
*
Control
Sora 1 μM
Sora 3 μM
Sora 5 μM
Sora 10 μM
HepG2
HepG2 AR

Figure 6. Rapid tumor growth in xenograft nude mice bearing Huh-BAT AR cells. Tumor growth rates of Huh-BAT AR cells were significantly higher than those of Huh-BAT cells (P=0.026).

Abbreviation: AR, anoikis resistant.

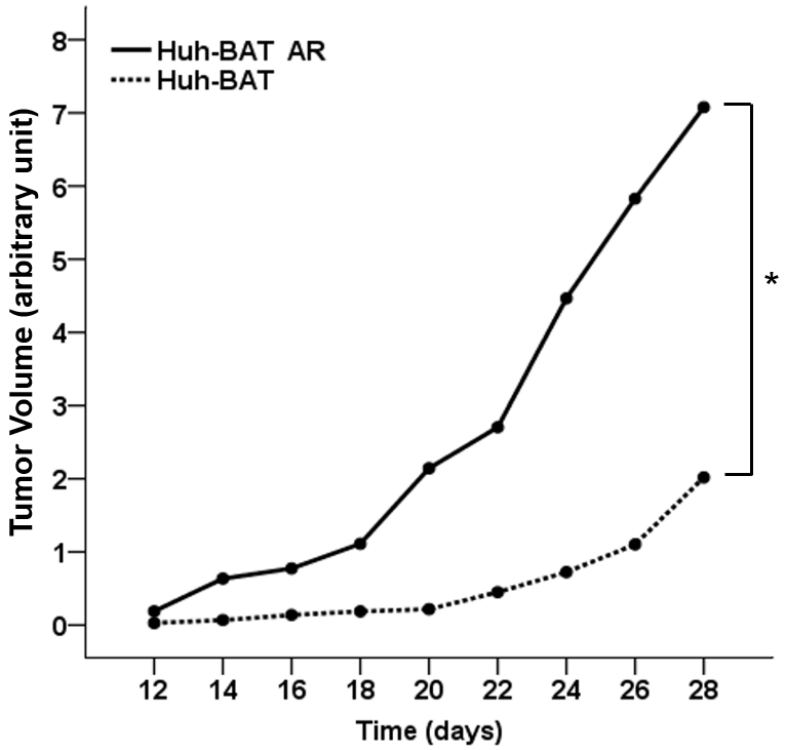

Figure 7. Expression of HK II and rGCS after 3-BP, BSO, and a combination treatment of 3-BP and BSO in Huh-BAT, HepG2, and corresponding AR cells. (A) Expression of HK II was decreased after 3-BP (40 μM) treatment and increased after BSO (200 μM) treatment; Expression of rGCS was increased after BSO (200 μM) treatment. (B) When treated with a combination treatment of 3-BP (40 μM) and BSO (200 μM), HK II expression was suppressed and rGCS expression was increased as compared to the control.

Abbreviation: AR, anoikis resistant; BSO, buthionine sulfoximine; CTL, control; HK II, hexokinase II; rGCS, gamma-glutamylcysteine synthetase; 3-BP, 3-bromopyruate.

(A)

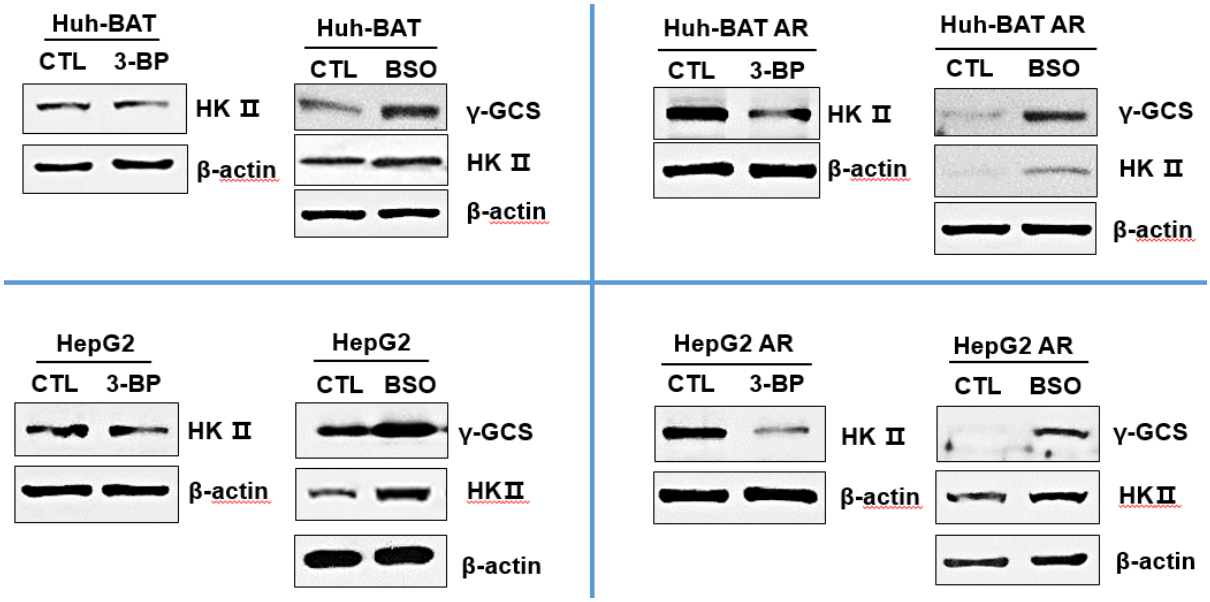

(B)

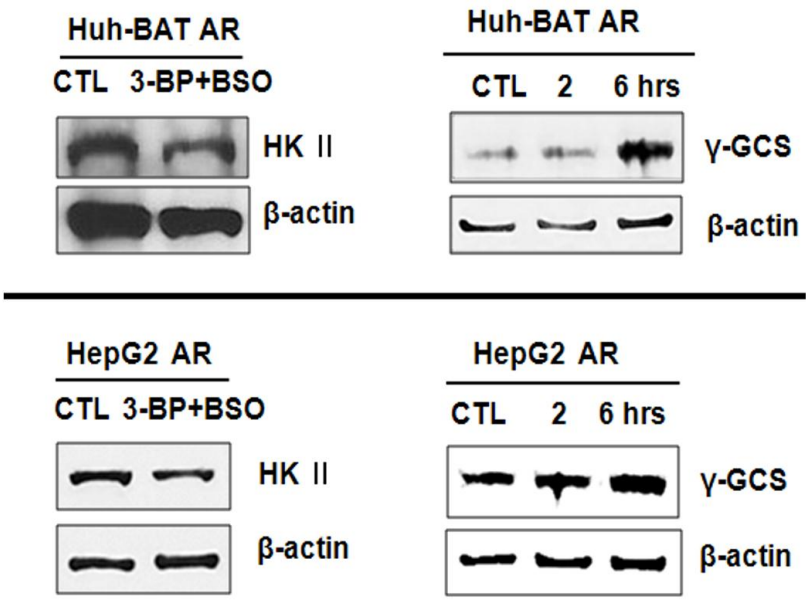
Huh-BAT AR
CTL 3-BP+BSO
HK II
β-actin
Huh-BAT AR
CTL 2 6 hrs
γ-GCS
β-actin
HepG2 AR
CTL 3-BP+BSO
HK II
β-actin
HepG2 AR
CTL 2 6 hrs
γ-GCS
β-actin

Figure 8. Suppression of glutathione production. Glutathione production was significantly suppressed after BSO or a combination treatment of 3-BP (40 μM) and BSO (200 μM) as compared to the control in Huh-BAT AR and HepG2 AR cells: P<0.001, BSO; P<0.001, a combination treatment for Huh-BAT AR cells and P=0.001, BSO; P=0.001, a combination treatment for HepG2 AR cells.

* means P<0.05; ** means P<0.01; *** means P<0.001

Abbreviation: AR, anoikis resistant; BSO, buthionine sulfoximine; 3-BP, 3-bromopyruate.

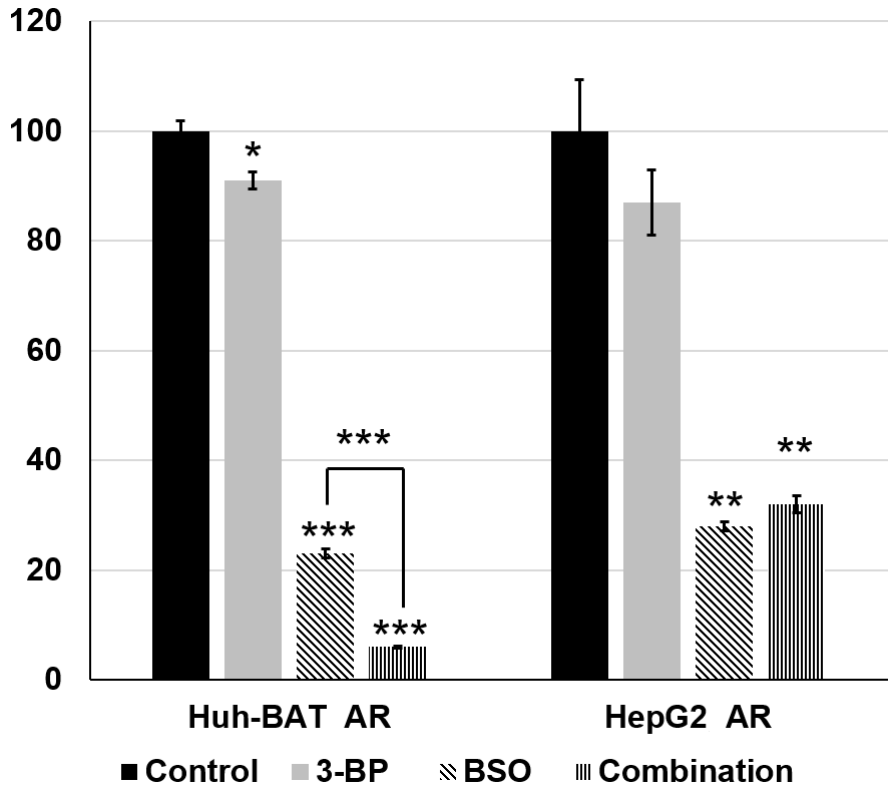

Figure 9. Change of ROS production by 3-BP (40 μM), BSO (200 μM), or a combination treatment of 3-BP and BSO. *In situ* fluorescence staining showed high enhancement in cells treated with the indicated treatment as compared to the control in Huh-BAT AR (A) and HepG2 AR cells (B). (C) ROS production was significantly increased at 3-BP (40 μM), BSO (200 μM), and a combination treatment of 3-BP (40 μM) and BSO (200 μM) as compared to the control (P=0.003, 3-BP; P=0.02, BSO; P=0.002, a combination treatment of 3-BP and BSO for Huh-BAT AR cells and P<0.001, 3-BP; P=0.008, BSO; P=0.003, a combination treatment of 3-BP and BSO for HepG2 AR cells).

Abbreviation: AR, anoikis resistant; BSO, buthionine sulfoximine; ROS, reactive oxygen species; 3-BP, 3-bromopyruate.

(A)

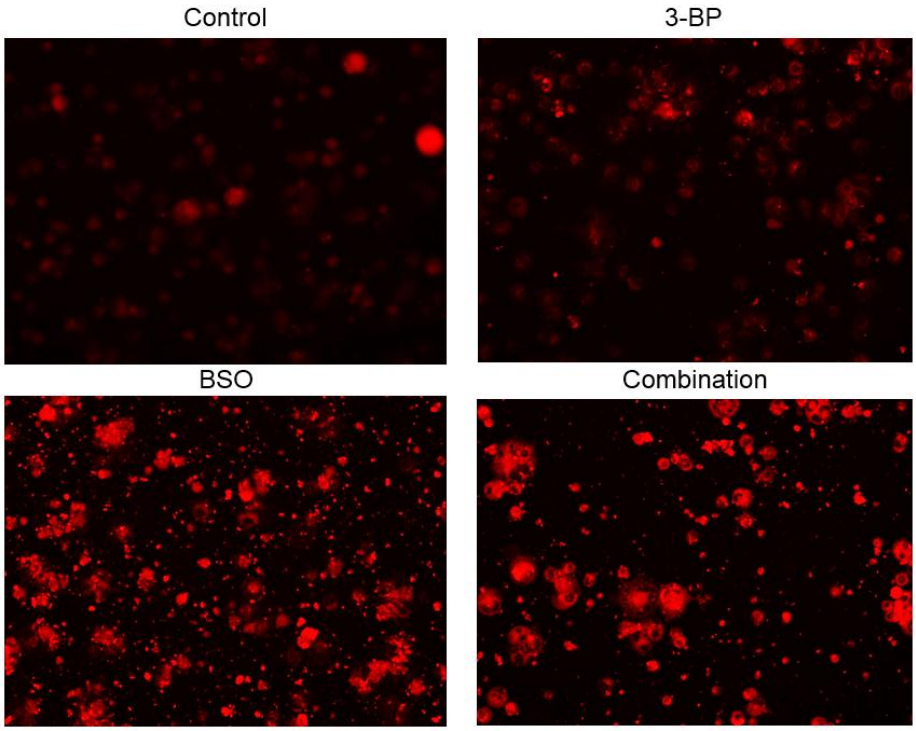

(B)

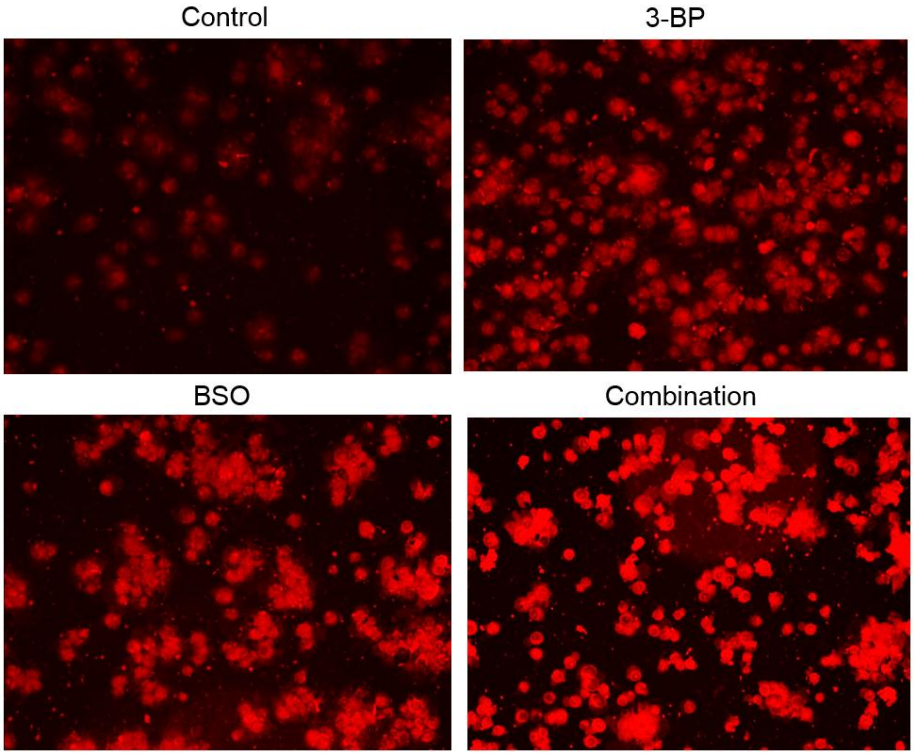
Control
3-BP
BSO
Combination

(C)

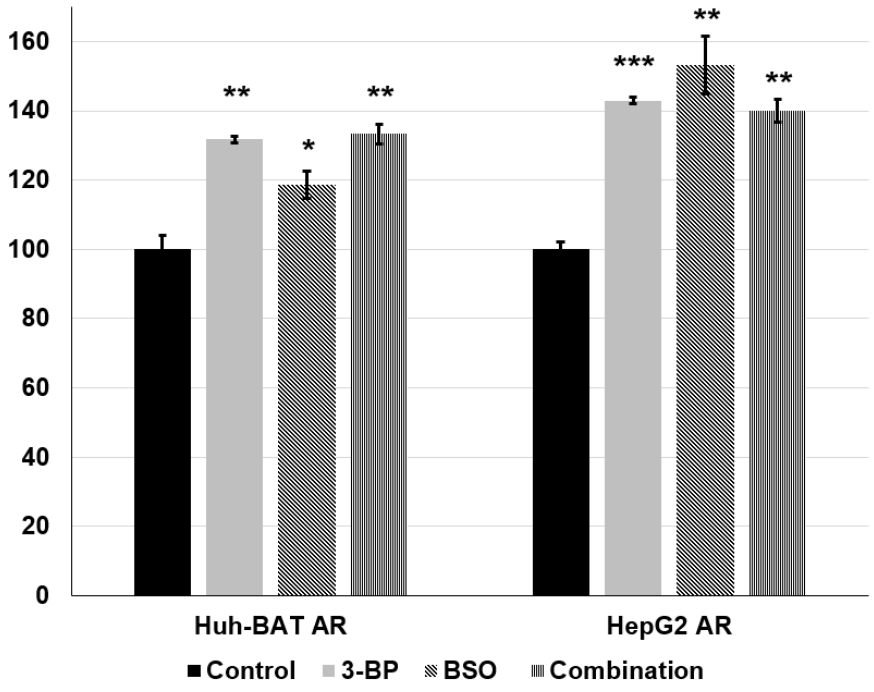
160
140
120
100
80
60
40
20
0
**
*
**
***
**
**
Huh-BAT AR
HepG2 AR
Control
3-BP
BSO
Combination

Figure 10. Change of lactic acid production by 3-BP (40 μM), BSO (200 μM), and a combination treatment of 3-BP and BSO. (A) Lactic acid production in Huh-BAT, HepG2, and corresponding AR cells was significantly suppressed after 3-BP (40 μM) treatment as compared to the control (P=0.038 in Huh-BAT; P<0.001 in Huh-BAT AR; P<0.001 in HepG2; P=0.002 in HepG2 AR cells). (B) Lactic acid production in Huh-BAT, HepG2, and corresponding AR cells was significantly increased after BSO (200 μM) treatment as compared to the control (P<0.001 in Huh-BAT; P<0.001 in Huh-BAT AR; P<0.001 in HepG2; P=0.001 in HepG2 AR cells). (C) Lactic acid production was significantly suppressed after a combination treatment of 3-BP (40 μM) and BSO (200 μM) in Huh-BAT AR and HepG2 AR cells; there was a significant difference among baseline, 2, and 12 hours exposure to a combination treatment (P<0.001 between baseline and 2 hours and P<0.001 between baseline and 12 hours exposure in Huh-BAT AR cells; P=0.042 between baseline and 2 hours and P=0.01 between baseline and 12 hours exposure in HepG2 AR cells).

* means P<0.05; ** means P<0.01; *** means P<0.001

Abbreviation: AR, anoikis resistant; BSO, buthionine sulfoximine; ROS, reactive oxygen species 3-BP, 3-bromopyruate.

Bars, SD.

(A)

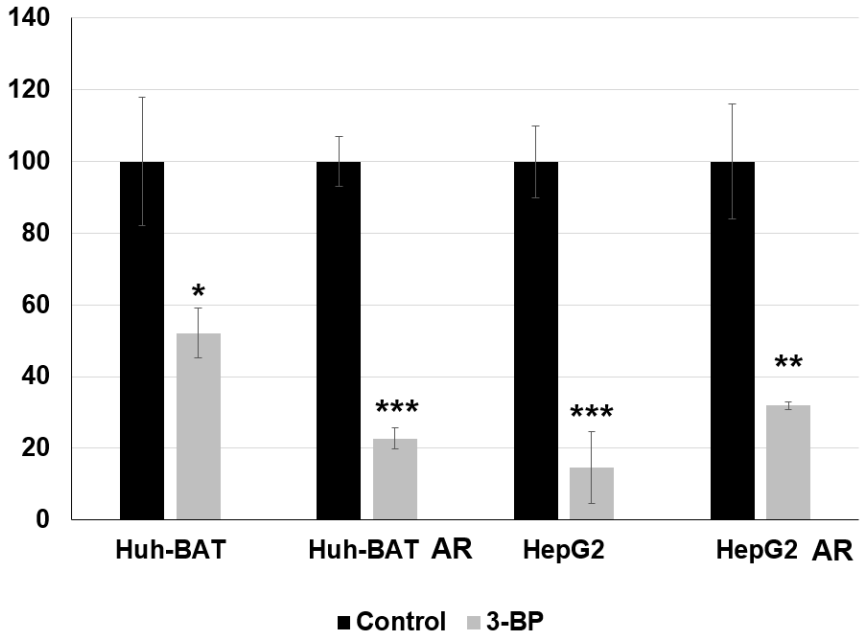
140
120
100
80
60
40
20
0
*
***
***
**
Huh-BAT
Huh-BAT AR
HepG2
HepG2 AR
Control
3-BP

(B)

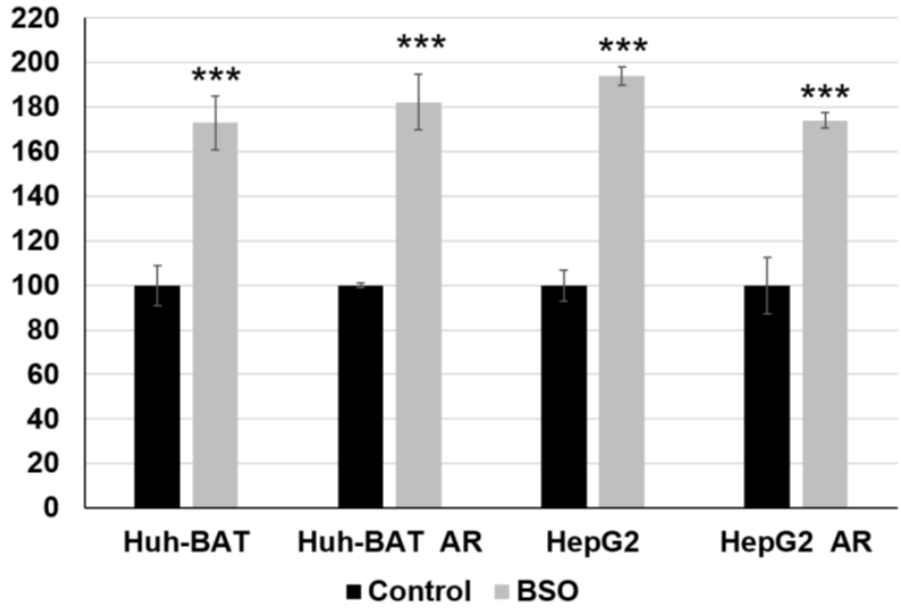
220
200
180
160
140
120
100
80
60
40
20
0
***
***
***
***
Huh-BAT
Huh-BAT AR
HepG2
HepG2 AR
Control
BSO

(C)

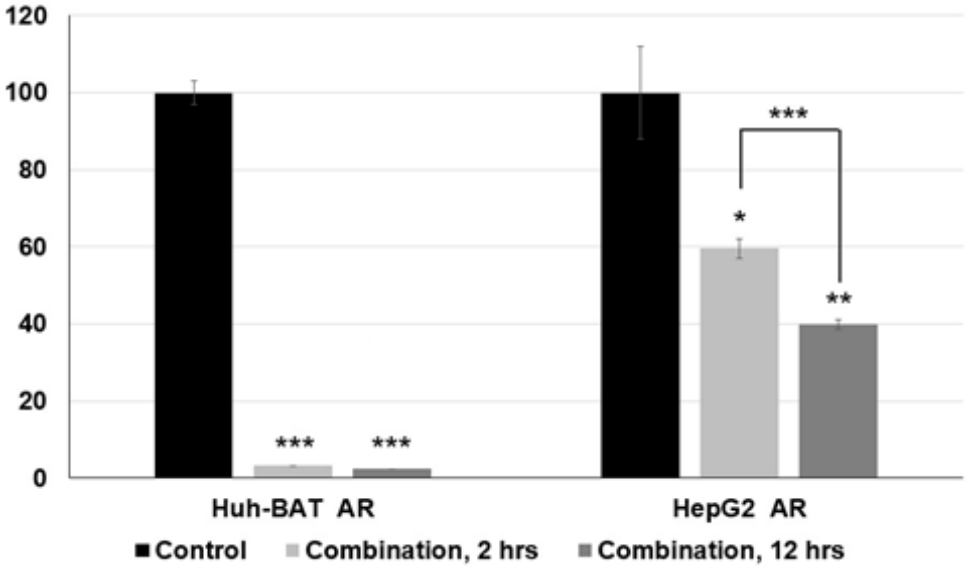
120
100
80
60
40
20
0
***
***
*
***
**
Huh-BAT AR
HepG2 AR
Control
Combination, 2 hrs
Combination, 12 hrs

Figure 11. Cell viabilities of Huh-BAT, HepG2, and corresponding AR cells after 3-BP or BSO treatment. (A) Viabilities of Huh-BAT and Huh-BAT AR cells were decreased after 3-BP treatment. (B) In Huh-BAT AR cells, cell viabilities at each concentration were significantly lower after BSO treatment as compared to those of Huh-BAT cells (all, P<0.05). (C) Viabilities of HepG2 AR cells showed significantly higher than those of HepG2 cells after 3-BP treatment (all, P<0.01). (D) In HepG2 and HepG2 AR cells, cell viabilities were not effectively suppressed after BSO treatment. At high concentration of 800 μM, BSO, viabilities of HepG2 AR cells were significantly suppressed as compared to those of HepG2 cells (P=0.04).

* means P<0.05; ** means P<0.01; *** means P<0.001

Abbreviation: AR, anoikis resistant; BSO, buthionine sulfoximine; 3-BP, 3-bromopyruate.

Bars, SD.

(A)

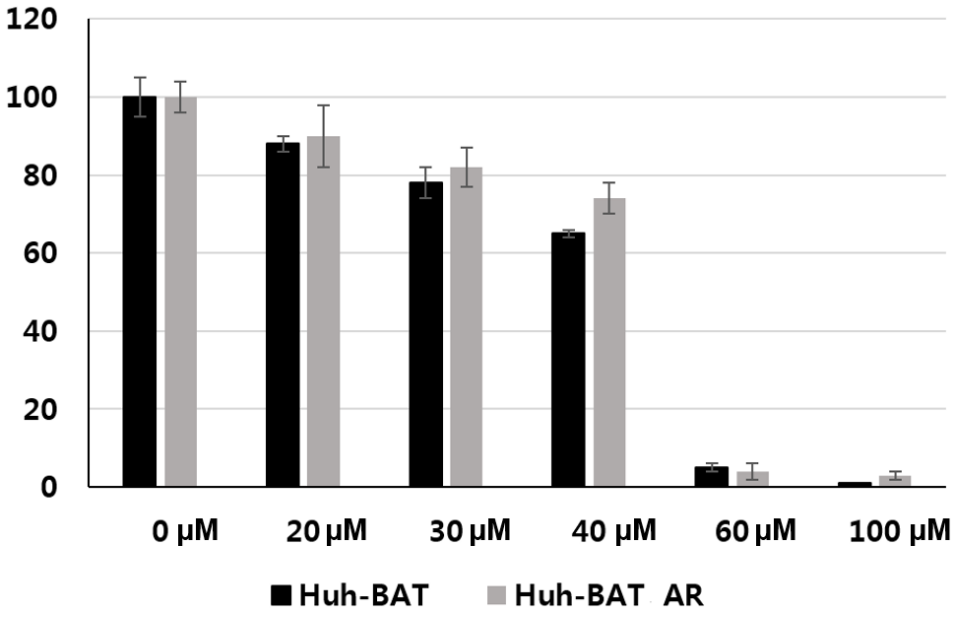

(B)

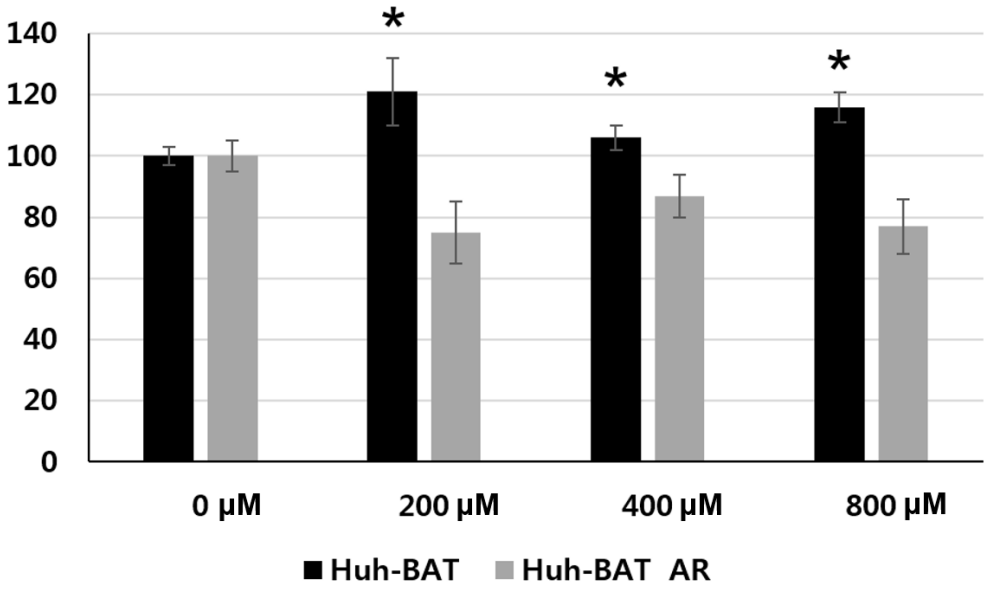
140
120
100
80
60
40
20
0
*
*
*
0 μM
200 μM
400 μM
800 μM
Huh-BAT
Huh-BAT AR

(C)

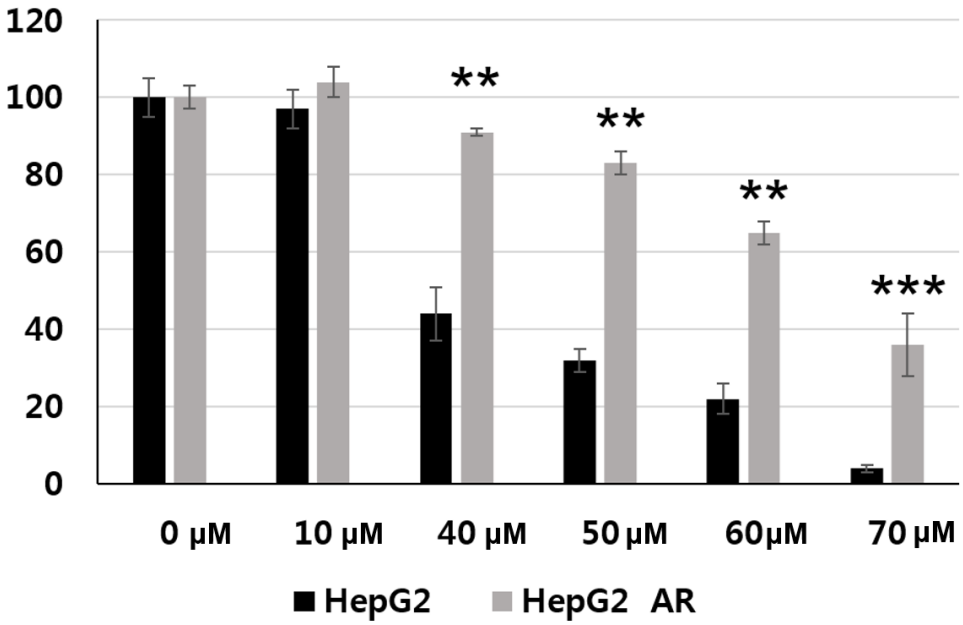
120
100
80
60
40
20
0
**
**
**
***
0 μM
10 μM
40 μM
50 μM
60μM
70 μM
HepG2
HepG2 AR

(D)

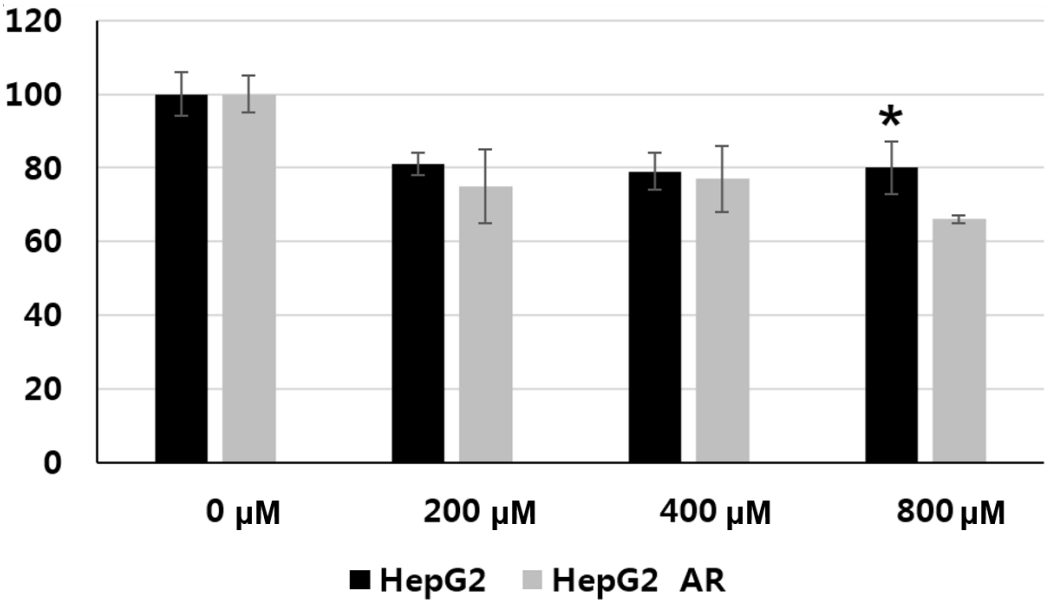

Figure 12. Cell viabilities of Huh-BAT, HepG2, and corresponding AR cells after a combination treatment of 3-BP and BSO. Viabilities of Huh-BAT and Huh-BAT AR cells (A), HepG2 and HepG2 AR cells (B) were effectively suppressed. Each concentration of 3-BP was treated 24 hours after 200 μM BSO treatment in those cells.

** means P<0.01

Abbreviation: AR, anoikis resistant; BSO, buthionine sulfoximine; 3-BP, 3-bromopyruate.

Bars, SD.

(A)

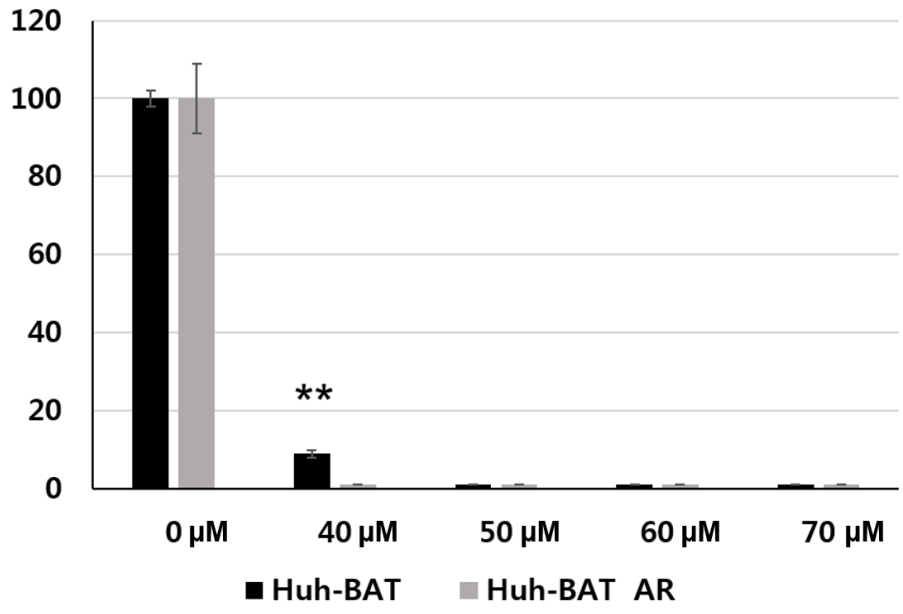

(B)

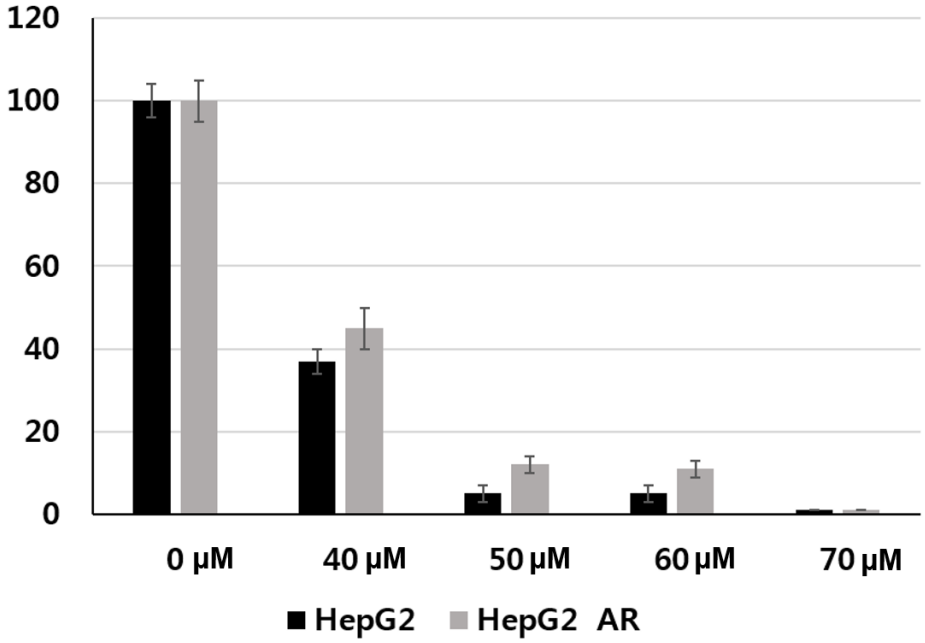

Figure 13. Apoptosis assay after 3-BP, BSO, and a combination treatment of 3-BP and BSO. Apoptosis rates of Huh-BAT, HepG2, and corresponding AR cells receiving the indicated treatments were evaluated by annexin V-FITC staining. The upper panel depicts the proportion of apoptotic cells, and the lower panel shows the quantitative results. A combination treatment of 3-BP and BSO significantly increased apoptosis rates as compared to the control (P=0.026 in Huh-BAT; P=0.001 in Huh-BAT AR; P=0.004 in HepG2; P=0.002 in HepG2 AR cells). When apoptosis rates were compared according to each treatment, a combination treatment of 3-BP and BSO showed higher apoptosis rates as compared to single treatment of 3-BP or BSO; P=0.012, 3-BP in Huh-BAT cells; P=0.002, BSO and P=0.001, 3-BP in Huh-BAT AR cells; P=0.001, BSO and P=0.002, 3-BP in HepG2 cells; P=0.002, BSO and P=0.001, 3-BP in HepG2 AR cells. 3-BP concentrations, 40 μM were used for Huh-BAT/Huh-BAT AR cells and 60 μM for HepG2/HepG2 AR cells; BSO concentrations, 200 μM were used for all indicated cell lines. * means $P<0.05$; ** means $P<0.01$

Abbreviation: AR, anoikis resistant; BSO, buthionine sulfoximine; 3-BP, 3-bromopyruate. Bars, SD.

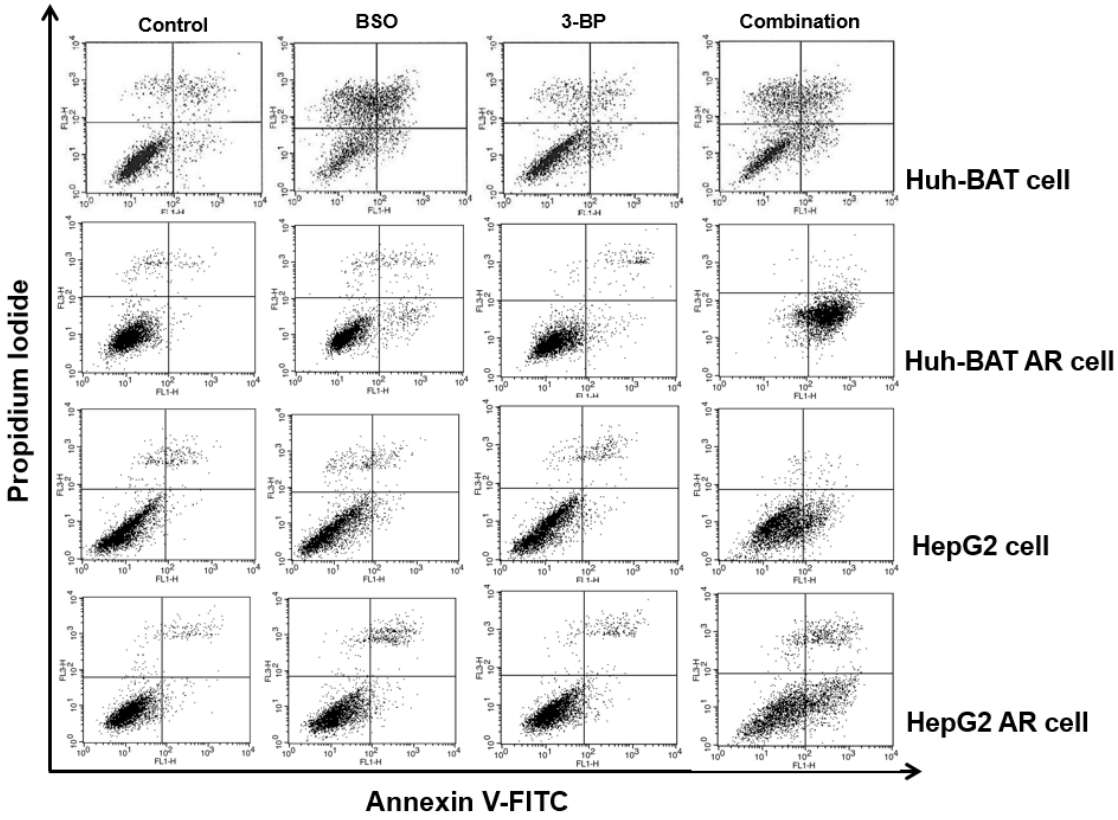
Control
BSO
3-BP
Combination
Huh-BAT cell
Huh-BAT AR cell
HepG2 cell
HepG2 AR cell
Propidium Iodide
Annexin V-FITC

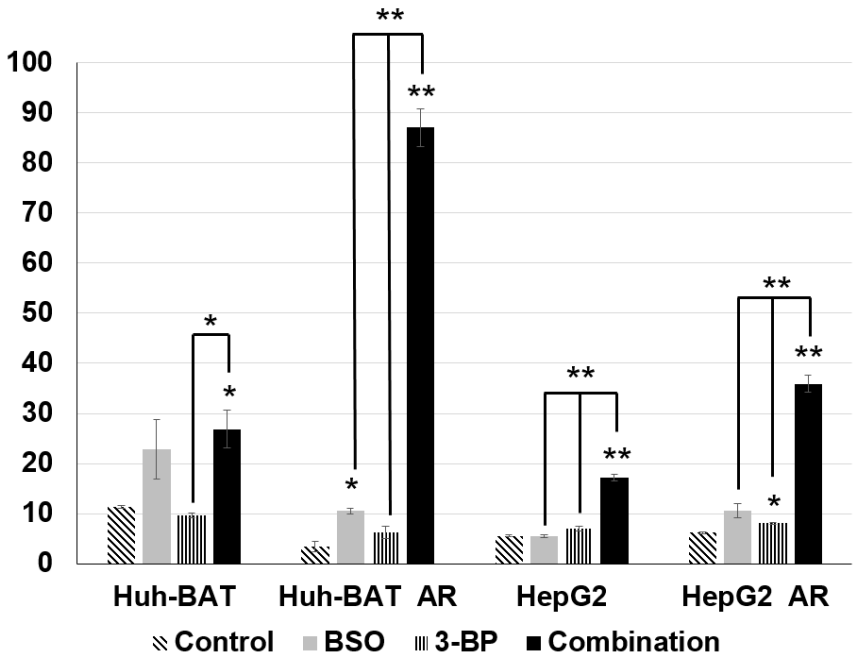
100
90
80
70
60
50
40
30
20
10
0
Huh-BAT
Huh-BAT AR
HepG2
HepG2 AR
Control
BSO
3-BP
Combination

Figure 14. Suppression of HCC invasion by 3-BP, BSO, a combination treatment of 3-BP and BSO. Invasion capability of Huh-BAT AR and HepG2 AR cells receiving the indicated treatments was examined by Boyden chamber assay (A and C) and the bar graph depicts quantification of migrated cells (B and D). Invasion capability of Huh-BAT AR (B) and HepG2 AR cells (D) receiving the indicated treatments was significantly lower from the control; the combined 3-BP (40 μM) with BSO (200 μM) treatment in either Huh-BAT AR or HepG2 AR cells significantly suppressed cell invasion as compared with the control (P=0.002, 3-BP; P=0.001, BSO; P=0.001, a combination treatment for Huh-BAT AR cell and P=0.006, 3-BP; P<0.001, BSO; P<0.001, a combination treatment for HepG2 AR cell).

* means P<0.05; ** means P<0.01; *** means P<0.001

Abbreviation: AR, anoikis resistant; BSO, buthionine sulfoximine; 3-BP, 3-bromopyruate.

Bars, SD.

(A)

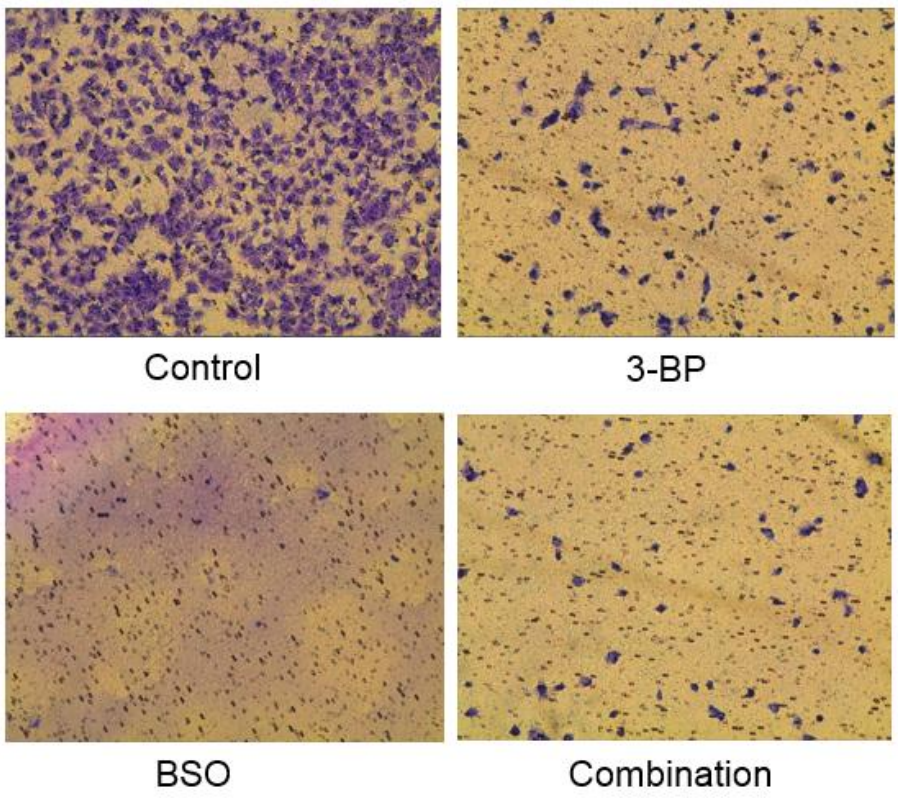

(B)

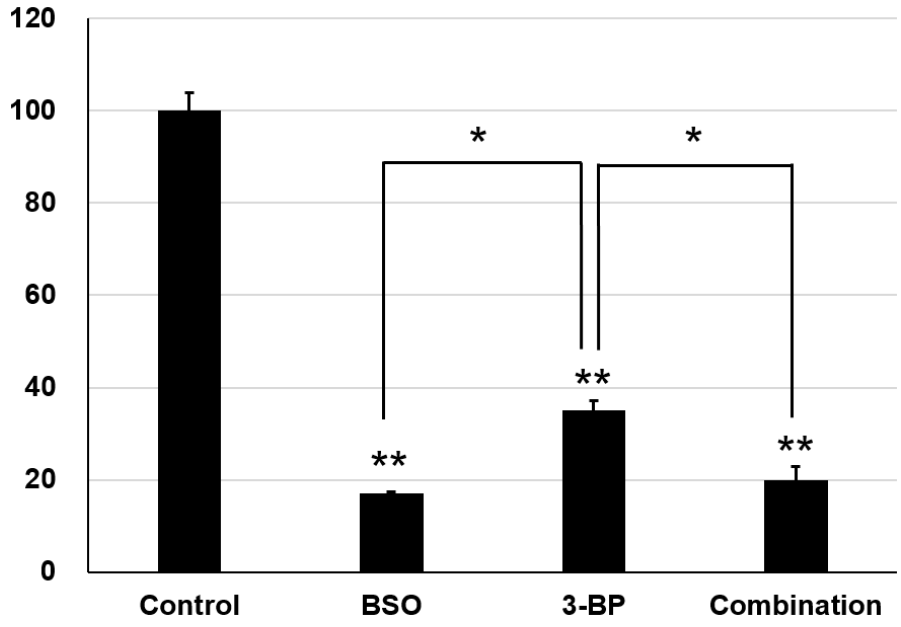
120
100
80
60
40
20
0
*
*
**
**
**
Control
BSO
3-BP
Combination

(C)

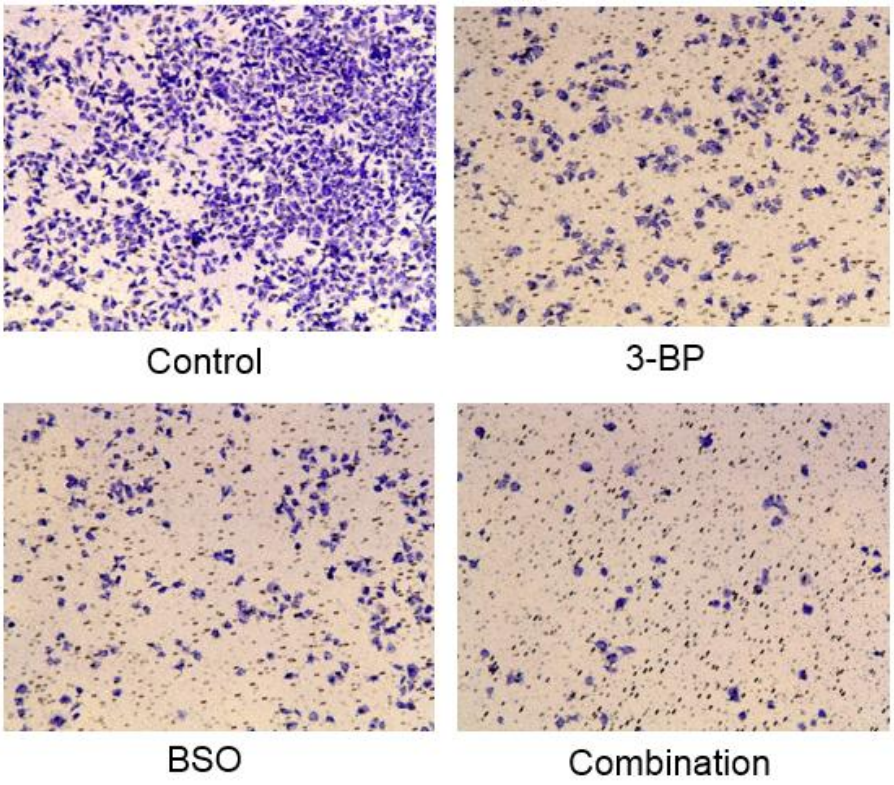
Control
3-BP
BSO
Combination

(D)

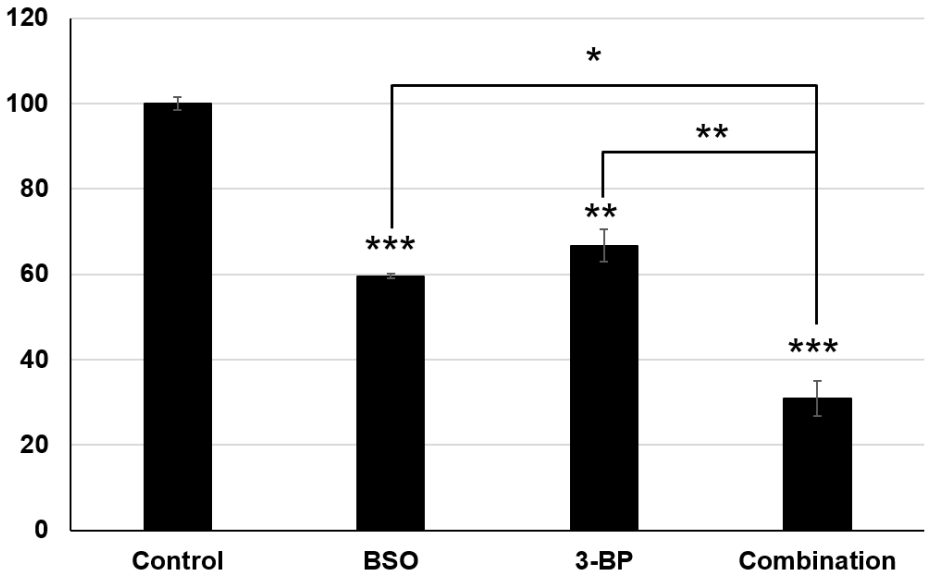

Figure 15. In vivo anti-tumor effects of 3-BP, sorafenib, and a combination treatment of 3-BP and BSO in xenograft nude mice bearing Huh-BAT AR cells. (A) Tumor growth rates in a combination treatment group were significantly lower than those in the control, sorafenib, or 3-BP treatment group (P=0.008, P=0.011, and P=0.013, respectively)(upper panel). There was no significant difference of tumor growth rates between the control and sorafenib treatment group (P=0.437), or between the control and 3-BP treatment group (P=0.243). Gross pictures of tumors before treatment, tumors grown in the control group, and tumors in a combination treatment group were shown (lower panel). (B) In vivo demonstration of the apoptosis-inducing efficacy in the control, 3-BP, sorafenib, and a combination treatment group was shown: H&E and TUNEL staining of tumor tissues in the control, sorafenib, 3-BP, and combination-treated mice (x 40 magnification). (C) TUNEL-positive cell percentages (apoptotic index) were determined in six different high power (x 400 magnification) fields. Apoptotic index was significantly higher in a combination treatment group as compared to other groups (P<0.001, the control group; P=0.001, the sorafenib treatment group; P=0.004, the 3-BP treatment group). (D) There was a significant difference of body weight between the control group and a combination treatment group (P=0.021).

* means P<0.05; ** means P<0.01; *** means P<0.001

Abbreviation: AR, anoikis resistant; BSO, buthionine sulfoximine; 3-BP, 3-bromopyruate.

Bars, SD.

(A)

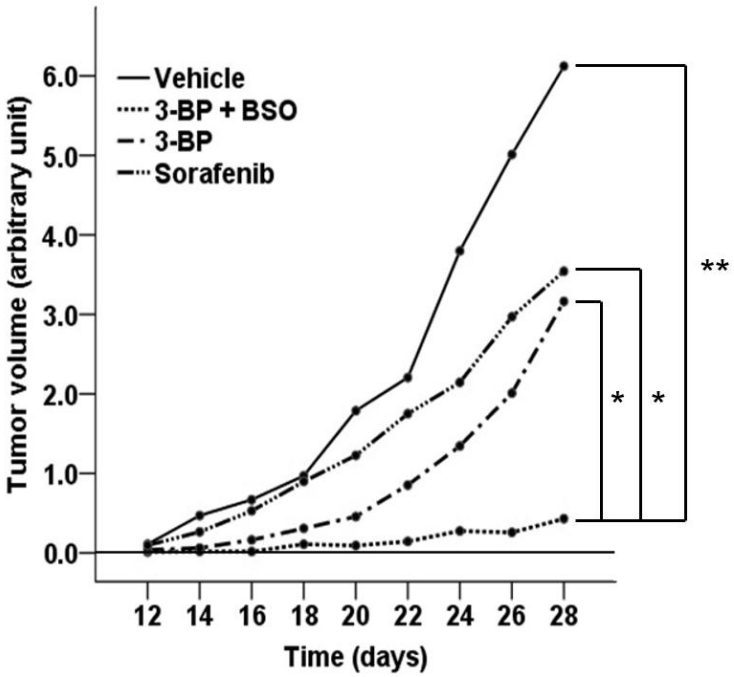
Vehicle
3-BP + BSO
3-BP
Sorafenib
Tumor volume (arbitrary unit)
6.0
5.0
4.0
3.0
2.0
1.0
0.0
12
14
16
18
20
22
24
26
28
Time (days)
**
*
*

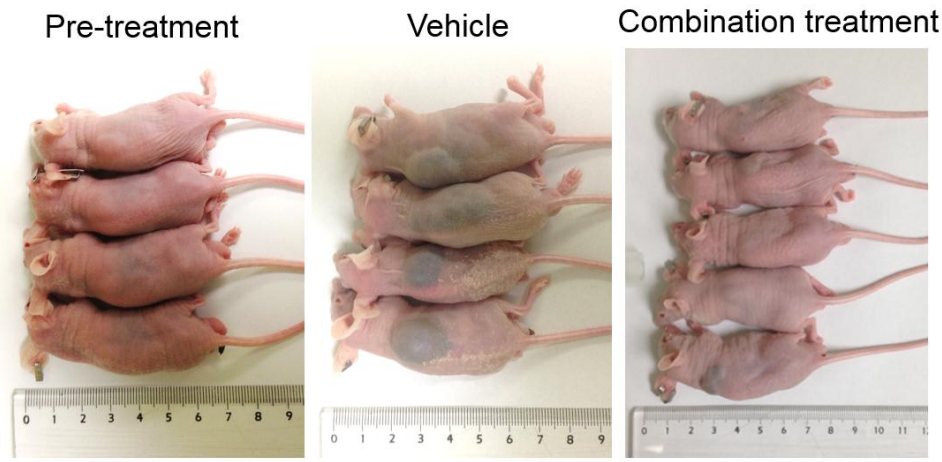
Pre-treatment
Vehicle
Combination treatment

(B)

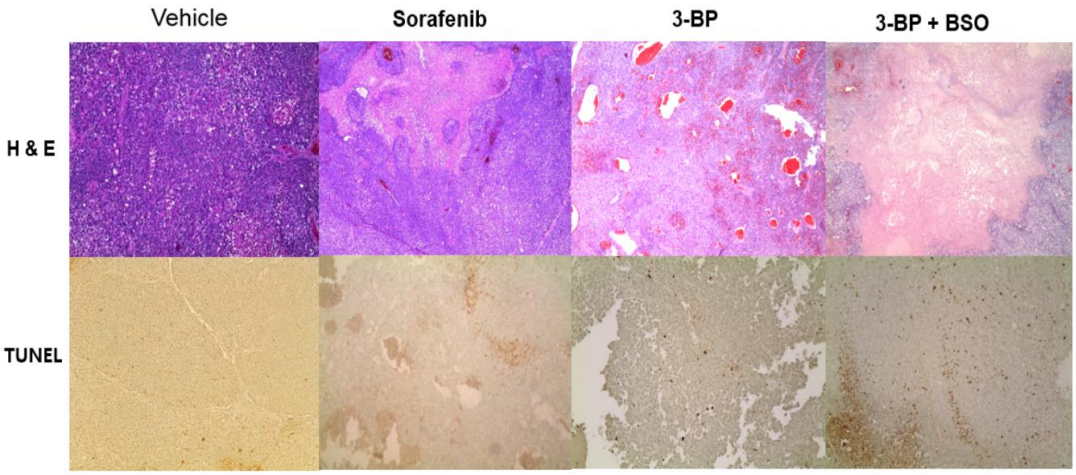
Vehicle
Sorafenib
3-BP
3-BP + BSO
H & E
TUNEL

(C)

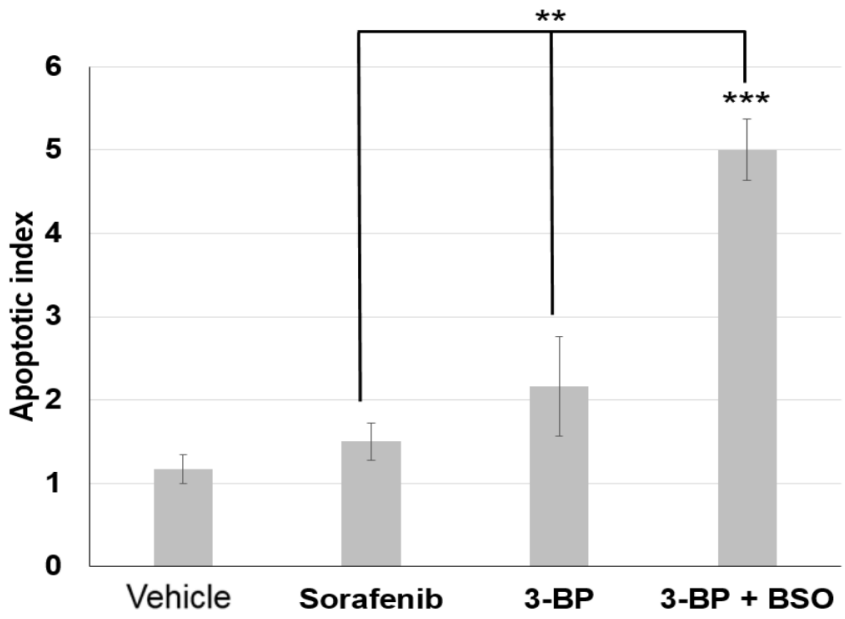
**
***
Apoptotic index
0
1
2
3
4
5
6
Vehicle
Sorafenib
3-BP
3-BP + BSO

(D)

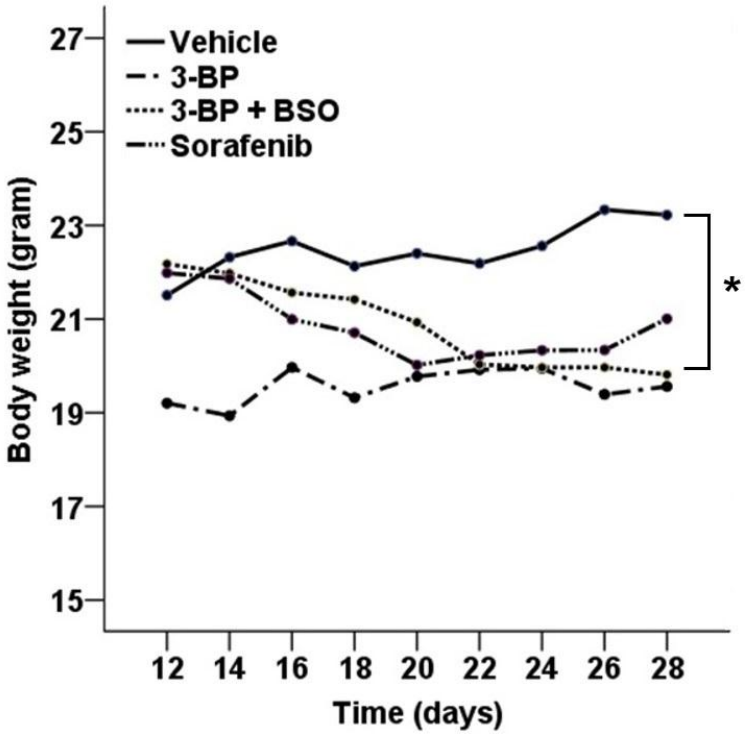
Vehicle
3-BP
3-BP + BSO
Sorafenib
Body weight (gram)
27
25
23
21
19
17
15
12
14
16
18
20
22
24
26
28
Time (days)
*

Figure 16. After matrix detachment, anoikis-resistant cancer cells decrease intracellular ROS levels through inducing enzymes involved in the glycolysis and antioxidant systems for their survival. The Warburg effect can be modulated by increased intracellular ROS levels. Increased ROS levels induce HK II expression and make cancer cells sensitive to 3-BP treatment, and thereby promote cell death via ROS-mediated apoptosis (the black box indicates monocarboxylate transporter 1, and the white box indicates monocarboxylate transporter 4).

Abbreviation: HK II, hexokinase II; ROS, reactive oxygen species; 3-BP, 3-bromopyruate.

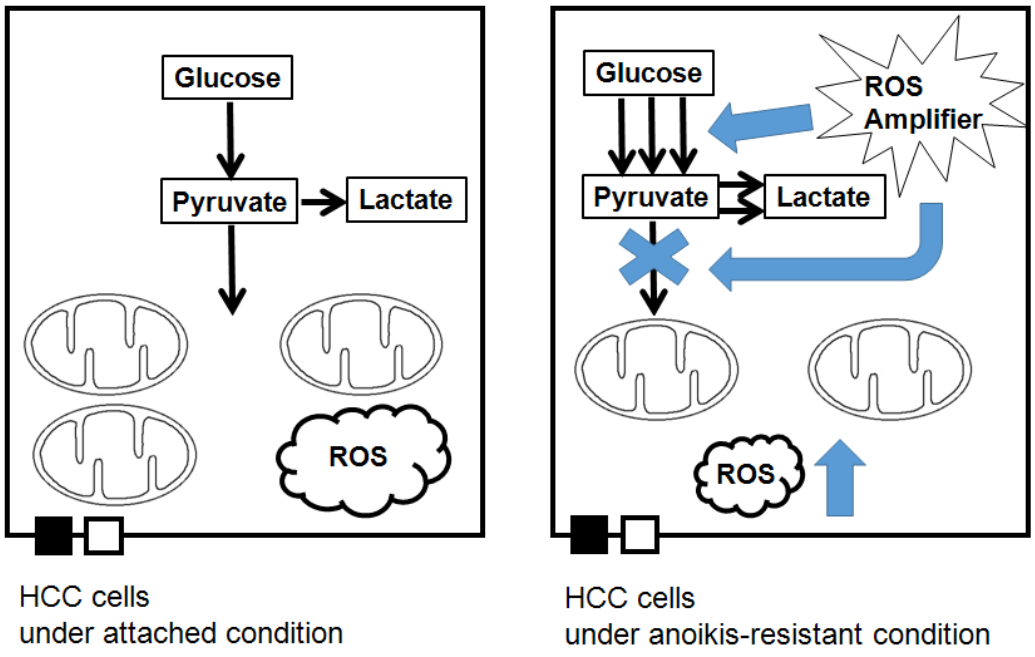

국문초록

목적: 간세포암 전이의 초기 단계에 있어서 아노이키스 저항성의 획득은 매우 중요하다. 그러나, 이러한 아노이키스 저항성을 보이는 간암세포에서 에너지대사와 항산화 시스템의 변화에 대해서 밝혀진 바가 없다. 본 연구에서는 아노이키스 저항성 간암세포 내 대사과정 및 항산화 시스템의 변화에 대해서 밝히고, 해당과정 억제제로 알려진 3-브롬화파이브릭산과 감마 글루타밀시스테인 합성효소의 억제제로 알려진 부사이노닌 설포시민의 상승적 항암효과에 대해서 규명해보고자 한다.

실험방법: 인체 간암유래 세포인 Huh-BAT와 HepG2 세포 및 이들로 유도된 아노이키스 저항성 세포를 이용하여 해당과정 및 활성산소의 발생을 측정하였다. 또한, 해당과정 및 항산화 시스템에 있어 핵심적 단백질인 헥소키나이제 II 와 감마 글루타밀시스테인 합성효소, 전이와 연관된 상피중간엽 세포이행과 관련된 단백질의 발현을 분석하였다, 헥소키나이제 II 억제제인 3-브롬화파이브릭산 및 감마 글루타밀시스테인 합성효소 억제제인 부사이노닌 설포시민을 상기 간암세포주에 처리하여 항암효과를 평가하였다. 누드 마우스 모델을 이용하여 상기 간암세포주를 이종이식한 뒤, 3-브롬화파이브릭산 및 부사이노닌 설포시민을 2주간 복강 내로 투약하면서 항암효과를 평가하였다.

결과: 아노이키스 저항성을 보이는 간암세포주는 부착형 간암세포주에 비하여 기존의 항암약물에 대한 약물저항성을 보였으며, 해당과정 및 항산화 시스템의 항진으로 보다 많은 젖산을 생산하고 보다 적은 활성화 산소를 생산하는 현상이 관찰되었다. 아노이키스 저항성을 보이는 간암세포주는 부착형 간암세포주에 비하

여 헥소키나이제 II 와 감마 글루타밀시스테인 합성효소, 상피중간엽 세포이행과 관련된 단백질의 발현이 증가하였다. 3-브롬화파이브릭산 및 부사이노닌 설포시민을 병합 투여하였을 때, 아노이키스 저항성 간암세포주의 세포자살을 통하여 세포사멸이 유도되었고 전이현상이 억제되었다. 이종이식된 누드 마우스 간암 모델에서도 아노이키스 저항성 간암의 성장이 효과적으로 억제되었으며, 이는 소라페닙 및 3-브롬화파이브릭산을 단독 투여하였을 때와 비교하여 보다 효과적으로 간암의 성장이 억제되었다.

결론: 아노이키스 저항성 간암 세포에서 3-브롬화파이브릭산 및 부사이노닌 설포시민의 병합투여는 상승적 항암효과를 보이며, 이러한 결과는 향후 소라페닙 치료에 저항성을 보이는 진행성 간암 환자의 치료에 있어 하나의 대안으로 제시될 수 있다.

핵심단어: 3-브롬화파이브릭산, 부사이노닌 설포시민, 간세포암, 아노이키스 저항성 세포

학번: 2014-30915